Drug metabolism activity is a Critical Intrinsic Selector for Hepatocytes to elongate cell lifespan by using a cell-killing antibiotic

Saeko Akiyama[1, 2], Noriaki Saku[1], Shoko Miyata[1], Kenta Ite[1], Masashi Toyoda[1,3], Tohru Kimura[4] , Masahiko Kuroda[5], Atsuko Nakazawa[1,6], Mureo Kasahara[7] , Hidenori Nonaka[1] , Akihide Kamiya[8] , Tohru Kiyono[9], Toru Kobayshi[10], Yasufumi Murakami[2], and Akihiro Umezawa[1*]

1 Center for Regenerative Medicine, National Center for Child Health and Development Research Institute, Tokyo, 157-8535, Japan
2 Tokyo University of Science, Tokyo, 125-8585, Japan
3 Research team for Geriatric Medicine (Vascular Medicine), Tokyo Metropolitan Institute of Gerontology, Tokyo, 173-0015, Japan
4 Laboratory of Stem Cell Biology, Department of BioSciences, Kitasato University School of Science, Kanagawa, 252-0373, Japan
5 Department of Molecular Pathology, Tokyo Medical University, 6-1-1 Shinjuku, Shinjuku-ku, Tokyo, 160-8402, Japan.
6 Saitama Children's Medical Center, Saitama, 330-8777, Japan
7 Organ Transplantation Center, National Center for Child Health and Development, Tokyo, 157- 8535, Japan
8 Department of Molecular Life Sciences, Tokai University School of Medicine, 143 Shimokasuya, Isehara, Kanagawa, 259-1193, Japan.
9 Project for Prevention of HPV-related Cancer, Exploratory Oncology Research and Clinical Trial Center, National Cancer Center, Chiba, 277-8577, Japan
10 Department of Strategy and Management, Clinical Research Center, National Center for Child Health and Development, Setagaya-ku, Tokyo, 157-8535, Japan

*Correspondence should be directed to:
Akihiro Umezawa,
Center for Regenerative Medicine
National Center for Child Health and Development Research Institute
2-10-1 Okura, Setagaya,
Tokyo, 157-8535, JAPAN
Phone: +81-3-5494-7047
Fax: +81-3-5494-7048
E-mail: umezawa@1985.jukuin.keio.ac.jp

ABSTRACT

The liver plays many important roles in homeostasis, including drug detoxification, metabolism, and bile production. Hepatocytes, which are the main constituent cells of the liver, play an important role in the pathogenesis of liver diseases, identification of candidate compounds in drug discovery research, pharmacokinetic studies, and toxicity evaluation. Human hepatocytes are, however, difficult to grow in normal in vitro culture systems, making it difficult to secure cell numbers. As an alternative, evaluation systems using animal models and hepatocellular carcinoma cells have been established, but interspecies and interracial differences and low hepatic function have been pointed out as problems. Therefore, there is still a need for a highly stable method to prepare human hepatocytes with sufficient functionality. In this study, we aimed to establish an in vitro long-term culture system that enables stable proliferation and maintenance of the functionality of human hepatocytes to stably supply human hepatocytes. In the established culture system, the stable proliferation of human hepatocytes was achieved by co-culturing hepatocytes with mouse fetal fibroblasts to dedifferentiate them into hepatic progenitor-like cells. Furthermore, we succeeded in purifying human hepatocytes by puromycin with a rapid cytocidal effect and proliferating them to over 30 population doublings for more than 200 days. Hepatocytes with high expression of cytochrome P450 genes survived after exposure to cytotoxic antibiotics because of enhanced drug-metabolizing activity. These results show that the above culture system enables simple and efficient hepatocyte proliferation, and is considered to be an effective method for stable supply of hepatocytes and significant cost reduction in drug discovery research.

INTRODUCTION

The liver is the largest metabolic organ in mammals and has more than 500 diverse functions, including glycogen storage, bile production, drug metabolism, ammonia metabolism, and detoxification. The liver is a collection of the smallest basic units called hepatic lobules, which are composed of bile duct epithelial cells, hepatocytes, hepatic stellate cells, Kupffer cells, and endothelial cells. Hepatocytes are parenchymal cells that account for about 80% of the organ and are responsible for liver functions. The morphological characteristics of hepatocytes include (1) large cell size with a diameter of about 20-30 μm, (2) round nuclei in the center of the cytoplasm, and (3) frequent multinucleation. It is also known that hepatocytes do not undergo mitosis under normal conditions, and the frequency of mitosis is said to be 1 in 1×10^5 to 2×10^5 cells [1].

Hepatocytes are very important as sources for cell transplantation and target cells for gene therapy, as well as for elucidating the pathogenesis of liver diseases and for drug discovery research [2–5]. Prediction of human-specific hepatotoxicity is important in drug discovery research, and inadequate prediction can lead to drug-induced liver injury (DILI), which can cause suspension of clinical trials [6]. Although laboratory animals and highly proliferative hepatocellular carcinoma cells are used in current drug discovery research, problems such as interspecies and interracial differences have been pointed out in these evaluation systems. Due to the wide range of hepatic functions, it is considered difficult to produce artificial substitutes, and therefore, a more accurate prediction of hepatotoxicity using human hepatocytes is required [5]. Hepatocytes are chronically scarce due to the following problems: (1) difficulty in securing available donor hepatocytes and (2) difficulty in vitro expansion [8,9]. Therefore, a highly efficient and stable method to prepare human hepatocytes with sufficient functionality needs to be developed.

Hepatocyte growth and culture systems based on liver regeneration mechanisms have been studied [7–9]. One of the characteristics of the liver is its high regenerative capacity, which is demonstrated when it is damaged by liver diseases or partial hepatectomy. Recent studies have shown that the dedifferentiation of bile duct epithelial cells and mature hepatocytes plays an important role in liver regeneration [8–12]. Specifically, it has been shown that hepatocytes and bile duct epithelial cells decidualize into highly proliferative hepatic progenitors in injured mouse livers, which are characterized by (1) a phenotype that is positive for both hepatocyte and bile duct epithelial markers, (2) characteristic cell morphology, and (3) high proliferative capacity [13–16]. Several reports are suggesting the presence of hepatic progenitors in the human diseased liver, and these cells maintain a morphologically and phenotypically intermediate state

between hepatocytes and bile duct epithelial cells, similar to the hepatic progenitors found in mice [9,11,17].

By constructing a culture system that mimics the findings of these liver regeneration mechanisms, it has been demonstrated that hepatic progenitor-like cells with proliferative potential can be induced from mouse or human mature hepatocytes in vitro [18–21]. Although the gene expression of markers is markedly reduced, it has been shown that hepatocytes can be induced to hepatic maturation by three-dimensional culture even after several passages. Therefore, it is suggested that the generation of hepatic progenitor-like cells using mature hepatocytes is an effective method for efficient and stable production and supply of human hepatocytes.

Puromycin is an aminonucleoside antibiotic produced by Streptomyces alboniger [22–24]. Puromycin is most commonly known as a selection marker for genetically modified cell lines and has also proven to be very useful as a probe for protein synthesis. Its structure is similar to that of the 3' end of aminoacyl-tRNA, and it can enter the A site of the ribosome and bind to the elongating strand, thereby inhibiting protein synthesis. This reaction, called puromycinylation, is known to be energy-independent and causes degradation of the 80S ribosome [24]. It has been suggested that the inhibition of the protein is non-specific and is a result of competition with aminoacyl-tRNA [23].

There is a shortage of available human hepatocytes, which are considered to be highly useful in drug discovery research and cell transplantation, and their widespread use requires a culture system capable of efficient, large-scale production of hepatocytes that maintain their functionality. The purpose of this study is to establish a long-term in vitro culture system that enables stable proliferation and maintenance of the functionality of human hepatocytes with the following three conditions: (1) establishment of cells with characteristics of hepatic progenitor-like cells, (2) maintenance of proliferation and functionality for a long time in vitro, and (3) induction of hepatic maturation by three-dimensional culture. We established the culture system that enables simple and efficient hepatocyte proliferation and is an effective method for a stable supply of hepatocytes in drug discovery research and cell transplantation.

MATERIALS AND METHODS

Ethical statement

All experiments handling human cells and tissues were approved by the Institutional Review Board at the

National Institute of Biomedical Innovation. Informed consent was obtained from the parent of the patient. Human cells in this study were utilized in full compliance with the Ethical Guidelines for Medical and Health Research Involving Human Subjects (Ministry of Health, Labor, and Welfare, Japan; Ministry of Education, Culture, Sports, Science and Technology, Japan). The derivation and cultivation of ESC lines were performed in full compliance with "the Guidelines for Derivation and Distribution of Human Embryonic Stem Cells (Notification of the Ministry of Education, Culture, Sports, Science, and Technology in Japan (MEXT), No. 156 of August 21, 2009; Notification of MEXT, No. 86 of May 20, 2010) and "the Guidelines for Utilization of Human Embryonic Stem Cells (Notification of MEXT, No. 157 of August 21, 2009; Notification of MEXT, No. 87 of May 20, 2010)". Animal experiments were performed according to protocols approved by the Institutional Animal Care and Use Committee of the National Research Institute for Child Health and Development.

Preparation of hepatocytes

Human hepatocytes were isolated from surplus liver tissue of a 1-year-old girl with DILI (Human hepatocyte 2064), a 7-month-old girl with DILI (Human hepatocyte 2061), a 1-month-old girl with DILI (Human hepatocyte 2062), a 7-month-old boy with DILI (Hep(C)/Hep2054)and a 9-month-old girl with DILI (Human hepatocyte 2055). Human primary hepatocytes were isolated according to the collagenase perfusion method [25–27]. First, liver tissues were shredded and washed with HEPES buffer (pH 7.7; 140 mM NaCl/2.68 mM KCl/0.2 mM Na_2HPO_4/10 mM HEPES). The tissues were then treated with 0.5 mg/mL collagenase/DMEM (Boehringer Mannheim) and diluted in the same buffer supplemented with 0.075% $CaCl_2$ at 37°C with gentle agitation. Cells were washed twice with HEPES buffer, 10% FBS, hEGF, transferrin, hydrocortisone, BSA, ascorbic acid, fungizone, 100 μg/ml penicillin-streptomycin, 5 μg/ml insulin, and 5×10^{-7} M hydrocortisone hemisuccinate. The cells were washed. Isolated cells were resuspended in HCM™BulletKit™ medium (Cat: CC-3198, LONZA) supplemented with hydrocortisone hemisuccinate (= Fresh MHs). The cells were cultured in medium (DMEM medium containing 20% FBS, 1% P/S) for 7-14 days, and then frozen at 2.2×10^6 cells per vial for future use (PHH2064, PHH2061, PHH2062, and PHH2055).

Human hepatocyte culture and passaging

Cryopreserved primary human hepatocytes (PHH2064, PHH2061, and PHH2062) were used. Frozen cells were thawed and seeded onto irradiated mouse embryonic fibroblasts (irrMEF) coated 60 mm dishes (BD Falcon 6-well plates) at a rate of 5×10^4 cells/cm2 (Passage 1). Then the cells were cultured in 37°C, Normoxia (5% CO_2 incubator) with ESTEM-HE medium (GlycoTechnica, Ltd., Japan) containing Wnt3a

and R-spondin 1 [28,29]. The medium was changed every 3 days. After 10-12 days of culture, the cells were trypsinized with 0.05% trypsin-EDTA (Sigma) and passages from 1-4 dishes during each passage.

Preparation of feeder cells

Mouse embryonic fibroblasts (MEF) were prepared for use as nutritional support (feeder) cells. Heads, limbs, tails, and internal organs were removed from E12.5 ICR mouse fetuses (Japan CLEA), minced with a blade, and seeded into culture dishes in a medium containing 10% FBS, 1% P / S to allow cell growth, and 1/100 (v/v) of 1 M HEPES buffer solution (INVITROGEN, 15630-106) was added to the cells. Following irradiation with an X-ray irradiation apparatus (Hitachi, MBR-1520 R-3; dose: 30 Gy), the cells were frozen using a TC protector (DS Pharma Biomedical, TCP-001).

Puromycin selection

For hepatocyte selection, puromycin (Wako, final concentration: 1 μg/mL or 2 μg/mL) was added to hepatocytes that had reached 90% confluence for 3 days. After exposure to puromycin, cells were washed with PBS and cultured in fresh ESTEM-HE for at least 1 day. When the cells reached 90% confluence, the cells were passaged by 0.25% trypsin-EDTA treatment.

human iPSC culture

iPSC-O cells were generated from fibroblasts derived from a patient with DILI (Human Hepatocyte No.2064) and iPSC-K cells were generated from fibroblasts derived from a patient with DILI (HepC) by the introduction of the Sendai virus carrying the 4 Yamanaka factors [30]. The iPSCs were cultured on irradiated mouse embryonic fibroblasts (irrMEFs) and medium for human iPSCs : KnockoutTM-Dulbecco's modified Eagle's medium (KO-DMEM) (Life Technologies, CA, USA; #10829-018) supplemented with 20% KnockoutTM-Serum Replacement (KO-SR; #10828-028), 2 mM Glutamax-I (#35050-079), 0.1 mM non-essential amino acids (NEAA; #11140-076), 50 U/ml penicillin-50 μg/ml streptomycin (Pen-Strep) (#15070-063), 0.055 mM β-mercaptoethanol (#21985-023) and recombinant human full-length bFGF (#PHG0261) at 10 ng/ml (all reagents from Life Technologies).

Hepatic differentiation of human iPSCs

For iPSC-K differentiation to hepatocyte-like cell (HLC-KI): To generate embryoid bodies (EBs), iPSC-K (1×10^4 cells/well) were dissociated into single cells with Accutase (Thermo Scientific, MA, USA) after exposure to the rock inhibitor (Y-27632: A11105-01, Wako, Japan), and cultivated in the 96-well plates in the EB medium [76% Knockout DMEM, 20% Knockout Serum Replacement (Life Technologies, CA,

USA), 2 mM GlutaMAX-I, 0.1 mM NEAA, pen-strep, and 50 µg/mL l-ascorbic acid 2-phosphate (Sigma-Aldrich, St. Louis, MO, USA)] for 10 days. The EBs were transferred to the 24-well plates coated with collagen type I and cultivated in the XF32 medium [85% Knockout DMEM, 15% Knockout Serum Replacement XF CTS (XF-KSR; Life Technologies), 2 mM GlutaMAX-I, 0.1 mM NEAA, Pen-Strep, 50 µg/mL l-ascorbic acid 2-phosphate (Sigma-Aldrich, St. Louis, MO, USA), 10 ng/mL heregulin-1β (recombinant human NRG-β 1/HRG-β1 EGF domain; R&D Systems, Minneapolis, MN, USA), 200 ng/mL recombinant human IGF-1 (LONG R3-IGF-1; Sigma-Aldrich), and 20 ng/mL human bFGF (Life Technologies)] for 35 days. For iPSC-O differentiation to hepatocyte-like cells (HLC-O): Hepatic differentiation of iPSC-O was performed by Cellartis Hepatocyte Differentiation Kit (TakaraBio, Y30051) following the manufacturer's instructions. In this study, cells at 30 days of differentiation induction were used.

Population doubling assay

Cells were harvested at sub-confluency and the total number of cells in each well was determined using a cell counter. Population doubling was used as the measure of cell growth. PD was calculated from the formula $PD=\log_2(A/B)$, where A is the number of harvested cells and B is the number of plated cells [31].

Histology and Periodic Acid Schiff (PAS) staining

Samples were coagulated in iPGell (GenoStaff) following the manufacturer's instructions and fixed in 4% paraformaldehyde at 4°C overnight. Fixed samples were embedded in a paraffin block to prepare cell sections. For HE staining, the deparaffinized sections reacted in a hematoxylin solution (Mutoh Chemical) for 5 minutes at room temperature and washed with dilute ammonia. After washing with 95% ethanol, dehydration was performed with 150 mL of eosin in 95% ethanol solution and permeabilized in xylene. For PAS staining, the deparaffinized sections were reacted with 0.5% periodate solution (Mutoh Chemical) for 10 minutes at room temperature, rinsed with water for 7 minutes. After reacting with Schiff's reagent (Mutoh Chemical) for 5-15 minutes, the sections were washed with sulfurous acid water. Coloration was done by reacting with Meyer hematoxylin solution (Mutoh Chemical) for 2 minutes at room temperature and then rinsing with water for 10 minutes.

Senescence Associated β-Galactosidase staining

For Senescence Associated b-Galactosidase staining, cells were fixed in 4% paraformaldehyde for 10 min at room temperature. Fixed cells were stained with the Cellular Senescence Detection Kit (Cell Biolabs, Inc.)

following the manufacturer's instructions.

Karyotypic analysis

Karyotypic analysis was contracted out to Nihon Gene Research Laboratories Inc. (Sendai, Japan). Metaphase spreads were prepared from cells treated with 100 ng/mL of Colcemid (Karyo Max, Gibco Co. BRL) for 6 h. The cells were fixed with methanol: glacial acetic acid (2:5) three times and placed onto glass slides (Nihon Gene Research Laboratories Inc.). Chromosome spreads were Giemsa banded and photographed. A minimum of 10 metaphase spreads was analyzed for each sample and karyotyped using a chromosome imaging analyzer system (Applied Spectral Imaging, Carlsbad, CA).

qRT-PCR

Total RNA was prepared using ISOGEN (Nippon Gene) and RNeasy Micro Kit (Qiagen). RNA was converted to cDNA using dNTP mix and Oligo (dT) by Superscript Ⅲ Reverse Transcriptase (Thermo Fisher). PCR was performed in ProFlex PCR System (Applied Biosystems). Quantitative RT-PCR was performed on QuantStudio 12K Flex (Applied Biosystems) using a Platinum SYBR Green qPCR SuperMix-UDG (Invitrogen). Expression levels were normalized with the housekeeping gene *UBC*. The primer sequences are shown in Table 2.

Immunofluorescence staining

Cells were fixed with 4% paraformaldehyde in PBS for 10 min at room temperature. After washing with PBS and treatment with 0.1% Triton X in PBS for 10 min, cells were pre-incubated with Protein Block Serum-Free (Dako) for 30 min at room temperature and then exposed to primary antibodies overnight at 4°C. Following washing with PBS, cells were incubated with diluted secondary antibodies for 30 min at room temperature. Nuclei were stained with DAPI (Biotium). For immunofluorescence staining in cut paraffin sections, sections were deparaffinized for 30 min before staining. Then sections were rinsed with distilled water for 3 min, and antigen retrieval was performed for 20 min using heated Histophine diluted 10 times with distilled water. After standing at room temperature for 20 min, sections were washed three times with PBS. Endogenous peroxidase removal was performed using 3% hydrogen peroxide water diluted 10 times with methanol for 5 min. After washing three times with PBS, sections were incubated with primary antibodies overnight at 4°C. After washing three times with PBS, sections were incubated with diluted secondary antibodies for 30 min at room temperature. Nuclei were stained with DAPI (Biotium). The antibodies listed in Tables 3 and 4 were diluted according to the table in DPBS containing 1% BSA.

Drug metabolizing enzyme induction

To examine the induction of drug-metabolizing enzymes, cells were cultured in 12-well plates (Falcon) using irrMEF and ESTEM-HE medium. When the cells reached 80-90% confluence, the following drugs were added to the cells: 20 μM rifampicin (solvent: DMSO) with an induction period of 2 days, 50 μM omeprazole (solvent: DMSO) with an induction period of 1 day, and 500 μM phenobarbital (solvent: DMSO) with an induction period of 2 days.

Measurement of CYP3A4 activity

For the measurement of CYP3A4 activity, cells were cultured in irrMEF and ESTEM-HE until 90% confluence. CYP3A4 activity was analyzed by P450-Glo CYP3A4 Assay and Screening System (Promega) following the manufacturer's instructions. HepG2 cells were used as a positive control.

Hepatic maturation by 3D culture

For hepatic maturation, the cells were detached with 0.25% trypsin/EDTA, transferred to 6-well plates at a density of 5×10^5 cells/well, and then cultivated for 10 days to form spheroids. Fresh medium was added 5 days after seeding and analysis was performed 10 days after transfer.

Microarray analysis

Microarray analysis including total RNA isolation was performed at DNA Chip Research (Japan). Briefly, total RNA was isolated using miRNeasy mini kit (QIAGEN). RNA samples were labeled and hybridized to a SurePrint G3 Human GEO microarray 8 × 60K Ver 3.0 (Agilent), and the raw data were normalized using the 75-percentile shift. For gene expression analysis, a one-way ANOVA was performed to identify differentially expressed genes (DEGs). murine s and fold-change numbers were calculated for each analysis (p-value < 0.05, fold-change>1.5). Unsupervised clustering was performed with sorted or whole DEGs using the R package (pheatmap, function: pheatmap()). Principal component analysis was performed with whole genes using the R package (function: prcomp()). Functional enrichment analysis including Over-Representation Analysis (ORA) and Gene Set Enrichment Analysis was performed by using WebGestalt (http://www.webgestalt.org/).

RESULTS

Propagation of human hepatocytes

We first examined human hepatocytes to investigate whether hepatocytes at a primary culture proliferate.

We isolated hepatocytes from the DILI patient's liver (Hep2064 cells) and assessed the proliferative capacity by culturing PHH (Figure 1A). Hepatocytes formed a colony a few days after seeding (Figure S1A) and proliferated until they reached confluence. After each passage, hepatocytes exhibited a colony-like morphology and continued growing until they became confluent (Figure 1B). Hepatocytes maintained their proliferative capacity for up to 200 days and proliferated nearly 10^{13} folds until 21 passages (Figure 1C). In early passages (~P6), hepatocytes showed small cell size and high nuclear-cytoplasmic ratio, but after several passages, the ratio of cytoplasm to nuclei became similar to that of hepatocytes. Hepatocytic cytoplasm became enlarged and stopped proliferation at 21 passages (Figure 1B). The proliferative marker Ki67 was positive at early passage (P5) but became negative at most cells at late passage (P21) (Figure 1E). SA-β-gal staining, a senescence marker, became strongly positive at 21 passages (Figure 1F). The karyotypic analysis revealed that hepatocytes with high proliferative capacity at P13 maintained a normal diploid karyotype, 46XX (Figure 1G).

We then analyzed the expression levels of the hepatocyte- and bile duct-associated genes. Hepatocytes expressed hepatocyte-associated genes such as ALB and AAT (Figure 2A). Hepatocytes showed decreased expression levels of the genes for ALB and CYP1A2. In contrast, hepatocytes showed increased expression of the genes for AAT and CYP3A4 during the first few passages and decreased expression in the later stages of passages. The expression of CK7 and CK19 varied, dependent on passage numbers (Figure 2A, S1B, and S1C). Immunocytochemistry revealed that hepatocytes expressed hepatocyte marker (ALB) and bile duct marker (CK7) in both the early and late passage (P5 and P21) (Figure 2B and 2D). Hepatocytic marker HNF4A was positive in the early passage (P5) but became negative in the late passage (P21) (Figure 2C). Also, binuclear cells were confirmed at P21 (Figure 2D, arrowheads). These results showed that hepatocytes had both biliary and hepatic characteristics and maintained a high proliferative capability for more than 200 days. Glycogen storage capacity was also confirmed at P21 when hepatocytes stopped dividing, but not at P3 and P13 (Figure 2E and 2F). We then evaluated hepatocytes for cytochrome P450 induction. We investigated expression levels of major three cytochrome P450 enzymes, CYP1A2, CYP2B6, and CYP3A4 (Figure 2G, H, I). We exposed the cells to omeprazole for 24 h, phenobarbital for 48 h, and rifampicin for 48 h. Expression of the CYP1A2 gene was up-regulated 21-fold upon exposure to omeprazole (Figure 2G); expression of the CYP2B6 gene was not induced with exposure to phenobarbital (Figure 2H); expression of the CYP3A4 gene was up-regulated 1.9- and 2.4-fold after exposure to rifampicin at P5 and P11, respectively (Figure 2I). CYP3A4 activity decreased along with the passages (Figure 2J).

Selection of proliferative hepatocytes by puromycin treatment

We hypothesized that hepatocytes have drug-metabolizing activity, including CYP3A4, which is responsible for detoxification and metabolism of antibiotics, and are resistant to antibiotics that kill mammalian cells. Based on this hypothesis, we exposed cultured hepatocytes to different concentrations of puromycin for 3 days to determine if the cultured hepatocytes were resistant to the antibiotic. The cultured hepatocytes showed resistance to puromycin at concentrations ranging from 1 μg/mL to 100 μg/mL (Figure 3B), while MEFs did not (Figure S2A). Hepatocytes selected with puromycin showed a small cell size and high nuclear-cytoplasmic ratio with clear nucleoli (Figure 3C). We then performed puromycin treatment on cultured hepatocytes from other DILI patients (#2061 and #2062) for reproducibility (Figure S2B, S2C, and S2D). The puromycin-selected hepatocytes (#2061 and #2062) exhibited almost the same morphology with Hep2064 cells. Gene expression analysis revealed that exposure to puromycin suppressed the expression of mesenchymal cell markers (COL1A1 and ASMA) and enhanced hepatocytic markers (ALB and AAT), drug-metabolizing enzyme genes (CYP1A2, CYP2B6, CYP3A4, and CYP2C9), and hepatic progenitor-associated markers (CK7, CK19, EpCAM, SOX9, and PROM1) (Figure S2E). Interestingly, the expression level of CPS1, a urea cycle-related enzyme, was suppressed when the expression level of drug-metabolizing enzyme genes was enhanced.

Next, we assessed the proliferative capacity of puromycin-treated cells (Figure 3D). The cells continued to proliferate to 60 population doublings for more than 350 days, in other words, the cells were propagated at nearly 10^{18} fold. The proliferating cells showed small cell size and high nuclear-cytoplasmic ratio in early passages (~P6), but after the sequential passages (~P20), the ratio of cytoplasm to nuclei became similar to that of hepatocytes. The cells increased homogeneity in population during the propagation from P5 to P20, and no senescence-like morphology such as significant cytoplasmic enlargement was observed. (Figure 3E and 3F). The cells in the early passage (P5) were positive for proliferative marker Ki67, but the number of Ki67-positive cells decreased in the late passage (P25) (Figure 3G). The cells at P25 started to have an activity of SA-β-gal, a senescence marker (Figure 3H). The karyotypic analysis showed that the cells at P24 maintained a normal karyotype, 46XX, after puromycin treatment (Figure 3I).

We examined the puromycin-selected cells after long-term culture for expression of hepatocyte- and bile duct-associated markers to investigate if the cells maintained their characteristics after long-term culture. The cells continued to express genes for hepatocyte and bile duct markers (Figure 4A and S3A). The expression levels of the genes for drug-metabolizing enzymes, which are CYP1A2, CYP2B6, and CYP3A4, became higher in the cells at the early passage (P4) after puromycin treatment (Figure 4B). Likewise, the

genes for hepatocytic markers such as ALB and AAT were up-regulated in the cells at P11 and P17. In contrast, the expression levels of mesenchymal cell markers significantly decreased with puromycin treatment, probably due to the elimination of mesenchymal cells and the selection of puromycin-resistant cells (Figure 4B). Along with gene expression, immunocytochemistry revealed that the cells expressed ALB and CK 7 in both early and late passages (P5 and P25, respectively) (Figure 4C and 4E). Hepatocyte marker HNF4A was positive in the early passage (P5), whereas negative in the late passage (P25) (Figure 4D). Binuclear cells of Hep2064 cells with puromycin treatment at P25 increased in number (Figure 4E). Glycogen storage was not detected in Hep2064 cells with puromycin with PAS staining (Figure 3F and 3G). The genes for CYP1A2 and CYP3A4 were significantly up-regulated by omeprazole and rifampicin, respectively (Figure 4H, I, J). Furthermore, the cells continuously exposed to puromycin maintained CYP3A4 activity (Figure 4K). We performed the same experiments in the cells with lower concentrations (1 μg/mL) of puromycin and obtained the same results in morphology, proliferation, and gene expression (Figure S4 and S5).

Global gene expression analysis

The global expression profiles were compared in human iPSC-derived hepatocyte-like cells and bile duct epithelial cells (Figure 5). Principal component analysis and hierarchical clustering analysis revealed that groups of "non-treatment" and "puromycin treatment" were clustered into independent groups, regardless of the passage numbers (Figure 5A). The Heatmap showed that the cells have both hepatocyte and bile duct characteristics in all passages (Figure 5B, 5C). To further elucidate the differences, we identified differentially expressed genes in PHH, Hep2064 cells, and Hep2064+px2 cells (Figure 5D). Compared with PHH, 3186 genes were significantly up-regulated in Hep2064 cells and 3551 genes in Hep2064+px2 cells, of which 3068 (83.6%) were coincidentally up-regulated (Figure 5E). Over-Representation Analysis was performed on the 3068 genes to identify the pathways that were significantly related to the genes (Figure 5E). We found that the cultured hepatocytes retained a hepatocyte-related gene expression pattern. Hep2064 and Hep2064+px2 cells showed enhanced expression of genes related to hepatocyte functions such as fatty acid metabolism, drug metabolism, amino acid degradation, and ammonium metabolism. We also identified enhanced expression of genes, related to ERBB signaling pathways which play an important role in liver regeneration and hepatocyte proliferation. Hep2064 and Hep2064+px2 cells exhibited significantly enhanced expression of fetal hepatobiliary hybrid progenitor and hepatic progenitor-related genes such as AFP, SOX9, PROM1, and EpCAM (Figure 5F, S6A, S6B, and S6C). Together, these results suggest that Hep2064 and Hep2064+px2 cells share common characteristics with hepatic progenitors. To elucidate the effect of puromycin, we compared gene expression of puromycin-treated and non-treated cells and

identified pathways by Gene Set Enrichment Analysis. The results showed that the enrichment of gene sets related to cell proliferation and division was much higher (FDR = 0.0, p-value = 0.0) in Hep2064+px2 cells than in Hep2064 cells, suggesting that Hep2064+px2 cells maintain a high proliferative capacity (Figure 5G). In addition to the DNA replication pathway, the amino acid degradation pathway, the fatty chain elongation pathway, and the oxidative phosphorylation pathway were identified as "enhanced pathways" (Figure 5H and S6D). Notably, the biosynthesis of ribosomes and tRNA, which is the active site of puromycin, was enhanced. This may indicate a homeostatic response of the cells to puromycin treatment. Furthermore, mitochondrial biosynthetic pathways were identified, suggesting that mitochondrial turnover may be enhanced in puromycin-treated cells (Figure 5I and S6E). Epithelial-mesenchymal transition core genes were enriched in Hep2064 cells (Figure S6F and S6G). Together, these results suggest that hepatic progenitors are purified by puromycin treatment through the removal of mesenchymal cells.

Hepatocyte Maturation

We next investigated whether Hep2064 and Hep2064+px2 cells could acquire reversible mature hepatocyte properties. We passaged Hep2064 and Hep2064+px2 cells at early (P5), middle (P11), and late (P21 or P25) passages, and cultured them in low attachment plates for 10 days in a three-dimensional (3D) culture (Figure 6A and S7A). Under 3D-culture conditions, Hep2064 and Hep2064+px2 cells formed spheroids irrespective of passages (Figure 6B-6D). Glycogen storage in Hep2064 and Hep2064+px2 cells, which could not be detected in 2D culture, was confirmed in 3D culture (Figure 6E-6J), and hepatocyte markers (ALB, CYP3A4, and MRP2) were expressed in 3D-cultured Hep2064 and Hep2064+px2 cells (Figure 6K-6M). Expression levels of hepatocyte markers, especially ALB, AAT, CYP1A2, CYP2B6, and CYP3A4, were significantly increased with maturation in 3D culture, whereas the expression of CK7, a bile duct, and progenitor-associated marker, was substantially suppressed (Figure 7A, 7B and 7C). It is noteworthy that the puromycin-induced hepatocyte maturation at both early and late passages in Hep2064 cells (Figure 7 and S8). These results suggest that Hep2064 and Hep2064+px2 cells regain characteristics close to mature hepatocytes and that the addition of puromycin is effective in maintaining the characteristics of mature hepatocytes.

DISCUSSION

Primary human hepatocytes, especially those derived from patients with liver diseases, are useful for elucidating pathological conditions and for drug discovery. However, despite the high availability of

hepatocytes, there is a chronic shortage of available hepatocytes due to their limited proliferative capacity. In this study, the establishment of a culture system to stably grow DILI patient-derived hepatocytes enabled us to elongate hepatocyte lifespan to more than 30 population doublings with the maintenance of hepatic progenitor progenitor-like phenotypes. Usage of Wnt3a/R-Spondin 1 in combination with the feeder cells for elongation of hepatocyte lifespan is in line with the previous report that WNTs are important for liver regeneration and in vitro propagation of hepatocytes and that irradiated MEFs are useful for maintaining the expression and proliferative capacity of hepatic progenitors [20,32,33].

As proof of its functionality, hepatocytes showed resistance to puromycin, an antibiotic metabolized in the liver, while rapid cell death was induced in MEFs and mesenchymal cells. This differential sensitivity to puromycin is probably due to the presence or absence of cytochrome P450 activity. Puromycin is metabolized mainly by CYP3A4 and can be confirmed based on the significant expression of CYP3A4. Puromycin, a commonly used antibiotic to select cells that are transduced with a puromycin-resistant gene, was useful for the selection of the proliferative biphenotypic hepatocytes and maintenance of the hepatic characteristics. Cells without metabolizing activity of the antibiotic are killed, but only functional hepatic progenitor cells or hepatocytes can metabolize the antibiotic and survive. Any antibiotic other than cell wall synthesis inhibitors may be used to select hepatocytes: Cell membrane function inhibitors, protein synthesis inhibitors, nucleic acid synthesis inhibitors, and folate synthesis inhibitors can be substituted. One type of antibiotic may be used alone, or a combination of two or more types may be used. Antibiotics that are commonly used for selecting stable transformants with exogenous genes can be used. Examples of antibiotics for selection include puromycin, blasticidin S, G418 (also known as GeneticinTM), hygromycin, bleomycin, and phleomycin (also known as ZeocinTM). Additionally, it is possible to isolate hepatocytes with the desired function by varying the type of additives that are specifically metabolized by hepatocytes. This functional selection method can be used like other conventional methods such as flow cytometry sorting and magnetic sorting.

When we explored the differences caused by the addition of puromycin, the biosynthesis of ribosomes and aminoacyl-tRNAs, which are the function sites of puromycin, were identified as gene sets that were enriched by Gene Set Enrichment Analysis. Puromycin promotes the degradation of the 80S ribosome [24,34] and the inhibition of protein synthesis by puromycin is due to competitive inhibition of aminoacyl t-RNA [35–37]. Besides, as a characteristic of puromycin, puromycin and its derivatives bind specifically to the stop codon of full-length proteins at low concentrations less than those at which they can compete effectively with aminoacyl-tRNA [23]. Therefore, in addition to the ability of hepatocytes to metabolize

drugs, puromycin resistance may be attributed to the stabilization of S80 ribosome and increased aminoacyl-tRNA levels.

Hepatic progenitors emerge after liver injury or partial hepatectomy and are mainly responsible for liver regeneration [38]. In these situations where mature hepatocytes with hepatic functions are decreasing, it is reasonable for hepatic progenitors to survive and proliferate with drug resistance to achieve rapid and efficient liver regeneration. Likewise, hepatocytes lose their proper characteristics after in vitro propagation [18–20]. The epithelial-mesenchymal transition may be involved in the reduced functionality of the propagated hepatocytes, and the reduced functionality may be avoided by removing mesenchymal cells and purifying hepatic progenitor cells. Inhibition of TGFβ signaling pathway that induces epithelial-mesenchymal transition is required for the hepatocyte culture system that maintains its function [39,40]. Successful recovery of hepatic function with the spheroid formation in this study indicates that the cells maintain a hepatic potential during the long-term propagation period. These results imply that propagation of hepatocytes and subsequent maturation with spheroid formation implement a large number of mature hepatocytes.

We herewith established an efficient and stable method for the selection and expansion of hepatic progenitor-like cells by utilizing a liver-specific drug-metabolizing function. This method may lead to the widespread use of cell transplantation by using a large number of hepatocytes. The propagated hepatocytes could have direct clinical applications to optimize technical and clinical aspects of cryopreservation and culture without the necessity to use viable natural hepatocytes. As an alternative for animal testing, the propagated hepatocytes may also upscale to robust platforms for drug discovery and toxicology to test the effect of environmental pollutants, chemical compounds, and pharmaceutical drugs on humans in the industrial sector. Finally, the cells can be used for understanding human genetic diseases such as DILI and correction of mutated genes in combination with the transduction of genome editing tools in the future.

Funding information

This research was supported by the Grant of National Center for Child Health and Development and Japan Agency for Medical Research and Development and AMED. Computation time was provided by the computer cluster HA8000/RS210 at the Center for Regenerative Medicine, National Research Institute for Child Health and Development.

Acknowledgments

We would like to express our sincere thanks to K. Miyado for fruitful discussion, to M. Ichinose and K. Tatsumi for providing expert technical assistance, to C. Ketcham for English editing and proofreading, and E. Suzuki and K. Saito for secretarial work.

Competing financial interests

AU is a co-researcher with MTI Ltd., Terumo Corp., BONAC Corp., Kaneka Corp., CellSeed Inc., ROHTO Pharmaceutical Co., Ltd., SEKISUI MEDICAL Co., Ltd., Metcela Inc., PhoenixBio Co., Ltd., Dai Nippon Printing Co., Ltd.. AU is a stockholder of TMU Science Ltd., Morikuni Ltd., and Japan Tissue Engineering Co., Ltd.. The other authors declare that there is no conflict of interest regarding the work described herein.

Figure Legends

Figure 1. Establishment of a long-term hepatocyte culture

A. Scheme of culture protocol.

B. Phase-contrast photomicrographs of hepatocytes (#2064) cells from passage 1, 5, 9, 13, and 21.

C. Growth curves of hepatocytes. Proliferative capacity was analyzed at each passage. Cells were passaged in the ratio of 1:4 for each passage (n=2). "Population doubling" indicates the cumulative number of divisions of the cell population.

D. Microscopic view of hepatocytes (#2064) at passages 3, 13, and 21. HE stain.

E. Immunocytochemical analysis of hepatocytes (#2064) with an antibody to Ki67 (cell proliferation marker).

F. A senescence-associated beta-galactosidase stain of hepatocytes (#2064) at the indicated passages. The number of β-galactosidase-positive senescent cells increased at passage 21.

G. Karyotypes of hepatocytes (#2064) at passage 13. Hepatocytes had 46XX and did not exhibit any significant abnormalities.

Figure 2. Characteristic analysis of hepatocytes (#2064) during long-term culture

A. Gene expression of hepatocytes (#2064) from passage 2 to 21 by qRT-PCR. Data were normalized with the housekeeping UBC gene. The expression level of each gene in passage 2 was set to 1.0. Error bars indicate the standard deviation (n=3).

B-D. Immunocytochemical analysis of hepatocytes (#2064) with antibodies to ALB (B), HNF4A (C), and bile duct marker CK7 (D) at the early and late passages (passage 5 and 21, respectively). Yellow arrows indicate binuclear cells (D).

E-F. Glycogen storage in hepatocytes (passage 3, 13, and 21) by PAS stain with (E) and without (F) diastase digestion.

G-I. Expression of the genes for CYP1A2 (G), CYP2B6 (H), and CYP3A4 (I) in hepatocytes after exposure to omeprazole (G), phenobarbital (H), or rifampicin (I). The expression level of each gene without any treatment (DMSO) was set to 1.0. Each expression level was calculated from the results of independent (biological) triplicate experiments. Error bars indicate standard error. The student's T-test was performed for statistical analysis of two groups. *$p < 0.05$, **$p < 0.01$, ***$p < 0.001$.

J. CYP3A4 activity of hepatocytes (passage 5, 11, and 21). The CYP3A4 activity of HepG2 cells was set to 1.0. Error bars represent the standard errors. Each expression level was calculated from the results of independent (biological) triplicate experiments. Error bars indicate the standard error. ***$p < 0.001$.

Figure 3. Puromycin-based selection of hepatocytes

A. Scheme of culture protocol. Puromycin was added at each passage for selection.

B. Phase-contrast photomicrographs of hepatocytes (#2064) with exposure of puromycin for 3 days. Different concentrations of puromycin (0, 1, 2, 10, 50 and 100 μg/mL) were added at 80% confluence.

C. Phase-contrast photomicrographs of hepatocytes (#2064) cells before and after 2 μg/mL puromycin. Puromycin was added when the cells reached confluence (Day 0) and removed 3 days after the addition (Day 3).

D. Growth curves of puromycin-treated hepatocytes (#2064) in duplicated experiments. Proliferative capacity was analyzed at each passage. Cells were passaged in the ratio of 1:4 at each passage (n=2). "Population doubling" indicates the cumulative number of divisions of the cell population.

E. Phase-contrast photomicrographs of puromycin-treated hepatocytes (#2064) at passage 5, 7, 13, 21, and 25.

F. Microscopic view of puromycin-treated hepatocytes (#2064) at passage 5, 13, and 25. HE stain.

G. Immunocytochemical analysis of puromycin-treated hepatocytes (#2064) with an antibody to Ki67 (cell proliferation marker).

H. A senescence-associated beta-galactosidase stain of puromycin-treated hepatocytes (#2064) at passages 5 and 25. The number of β-galactosidase-positive senescent cells increased at passage 25.

I. Karyotypes of puromycin-treated hepatocytes (#2064) at Passage 24. Details are given in Supplemental Figure S3B.

Figure 4. Characteristic analysis of puromycin-selected hepatocytes during long-term culture

A. Gene expression by qRT-PCR in puromycin-treated hepatocytes (#2064) from passage 4 to 25. Data were normalized with the housekeeping UBC gene. The expression level of each gene in passage 2 was set to 1.0. Error bars indicate the standard deviation (n=3).

B. Gene expression by qRT-PCR in puromycin-treated hepatocytes (#2064) at passages 4, 11, and 17 by qRT-PCR. Puromycin-treated ("Puro") and non-treated ("Non") hepatocytes (#2064) at passages 4, 11, and 17 were compared. The data were normalized by the housekeeping UBC gene. The expression level of each gene in passage 2 was set to 1.0. Error bars indicate the standard deviation. Each expression level was calculated from the results of independent (biological) triplicate experiments. The student's T-test was performed for statistical analysis of two groups. *$p < 0.05$, **$p < 0.01$, ***$p < 0.001$.

C-E. Immunocytochemical analysis of puromycin-treated hepatocytes (#2064) with antibodies to ALB (C), HNF4A (D), and bile duct marker CK7 (E) at the early and late passages (passage 5 and 25, respectively). Yellow arrowheads indicate binuclear cells (E).

F-G. Glycogen storage in puromycin-treated hepatocytes (passage 5, 13, and 25). (F) PAS stain. (G) PAS stain with diastase digestion.

H-J. Expression of the genes for CYP1A2 (H), CYP2B6 (I), and CYP3A4 (J) in puromycin-treated hepatocytes after exposure to omeprazole (H), phenobarbital (I), or rifampicin (J). The expression level of each gene without any treatment (DMSO) was set to 1.0. Each expression level was calculated from the results of independent (biological) triplicate experiments. Error bars indicate standard error (n=3). The student's T-test was performed for statistical analysis of two groups. *$p < 0.05$, ***$p < 0.001$.

K. CYP3A4 activity of hepatocytes (passage 5, 11, and 25). The CYP3A4 activity of HepG2 cells was set to 1.0. Error bars represent standard errors (n=3). Each expression level was calculated from the results of independent (biological) triplicate experiments. Error bars indicate the standard error. NS : $p>0.05$.

Figure 5. Global gene expression analysis of hepatocytes reveals a distinct hepatocyte group with the proliferative capability

A. Principal-component analysis (PCA) for non-treated hepatocytes (Non, #2064) at passage 1, 3, 6, 15, and 21), puromycin-treated hepatocytes (Puro, #2064) at passage 5, 15, and 25, PHH (PHH2064 and PHH2055), mature hepatocytes (Fresh MH), bile duct epithelial cells (GSM4454532, GSM4454533, GSM4454534), and iPSC-derived hepatocyte-like cells (HLC-O and HLC-KI) by global gene expression. Right: Hierarchical clustering analysis of expression profiles of the samples shown in PCA.

B-C. Heatmaps of the liver-associated genes. Genes up-regulated in mature hepatocytes (B) and bile duct epithelial cells (C) were used for the heatmap analysis (gene list: https://www.nature.com/articles/s41467-019-11266-x). The average gene expression in non-treated and puromycin-treated hepatocytes (#2064) was set to 0. Their expression levels were compared in groups of mature hepatocytes (Fresh MH), primary hepatocytes (PHH), and bile duct epithelial cells (BEC). The color bar indicates the signal intensity at log2 expression.

D. A heatmap for differentially expressed genes ($1.5 <$ fold changes and $p < 0.05$) in the comparisons of PHH versus non-treated hepatocytes (#2064) versus puromycin-treated hepatocytes (#2064). The color bars show the signal strength scaled by the z score.

E. Up-regulated genes ($1.5 <$ fold changes and $p < 0.05$) in non-treated and puromycin-treated hepatocytes (#2064) compared to PHH. Among the identified genes, 3,068 genes (83.6%) were matched. Bar graph: Over-Representation Analysis (ORA) of 3,068 genes with WebGestalt (WEB-based Gene SeT AnaLysis Toolkit) (FDR < 0.05).

F. Heatmap showing the expression levels of top fetal hepatobiliary hybrid progenitor up-regulated genes (gene list: https://www.nature.com/articles/s41467-019-11266-x) in PHH, non-treated and puromycin-treated hepatocytes (#2064). The color bars show the signal strength scaled by the z score.

G. Gene Set Enrichment Analysis was performed to identify enriched gene sets in puromycin-treated

hepatocytes (#2064) compared to non-treated hepatocytes (#2064) (FDR=0.0).

H. The top 15 gene sets enriched in puromycin-treated hepatocytes. Gene sets that were significantly upregulated in puromycin-treated hepatocytes (#2064) compared to non-treated hepatocytes (#2064) were clustered by affinity propagation method (FDR < 0.05) and ranked based on the normalized enrichment score1 (NES).

I. Gene sets related to mitochondrial biogenesis (FDR < 0.05) were enriched in puromycin-treated hepatocytes (#2064), compared to non-treated hepatocytes (#2064).

Figure 6. Spheroid formation induces hepatic maturation

A. Schematic of hepatic maturation protocol. Non-treated and puromycin-treated hepatocytes (#2064) at passage 5, 11, and 21 or 25 were cultured as spheroids for 10 days. See Figure S6A for details.

B-J. Histology of spheroids generated from non-treated hepatocytes (Non) and puromycin-treated hepatocytes (Puro) at early passage (B, E, F: passage 5), middle passage (C, G, H: passage 11), and late passage (D, I, J: passage 21 or 25). B, C, D: HE stain. E, G, I: PAS stain. F, H, J: PAS stain with diastase digestion.

K-M. Immunohistochemistry of spheroids generated from non-treated hepatocytes (Non) and puromycin-treated hepatocytes (Puro) at early passage (K: passage 5), middle passage (L: passage 11), and late passage (passage 21 or 25).

Figure 7. Hepatocytes restore the level of liver-associated gene expression after long-term cultivation to the level at the early stages of hepatocytic culture

Gene expression levels were analyzed by qRT-PCR. Non-treated and puromycin-treated hepatocytes (#2064) at passage 5 (A), 11 (B), and 21 or 25 (C) were applied to spheroid culture for 10 days (Figure S6A). The data were normalized by the housekeeping UBC gene. The expression level of each gene in passage 2 was set to 1.0. Error bars indicate the standard error. Each expression level was calculated from the results of independent (biological) triplicate experiments. The student's T-test was performed for statistical analysis of two groups. *$p < 0.05$, **$p < 0.01$, ***$p < 0.001$.

Supplemental Figure Legends

Supplemental Figure 1. Details of the morphology and gene expression of hepatocytes (#2064), related to Figures 1 and 2.

A. Phase-contrast photomicrographs of primary human hepatocytes (#2064) on irrMEF for 7 days. Two colonies are shown at low and high magnifications.

B. Gene expression by qRT-PCR in human hepatocytes (#2064) at passage 1 and 2. The data were normalized with the housekeeping UBC gene. Each relative value was calculated with respect to human hepatocytes (#2064) at the 2nd passage. Error bars indicate the standard deviation (n=3). "HepG2" cells, “Ad_Liver (human adult normal liver pools of five donors purchased from BioChain, R1234149-P)", and “Fresh_MH” (hepatocytes isolated from the adult human liver in our laboratory) are used for comparison.

C. Gene expression by qRT-PCR in hepatocytes (#2064) from passage 2 to 21. The data were normalized with the housekeeping UBC gene. The expression level of each gene in passage 2 was set to 1.0. Error bars indicate the standard deviation (n=3).

Supplemental Figure 2. Evaluation of the effect of puromycin on mouse fetal fibroblasts (MEF) and hepatocytes derived from other DILI patients, related Figure 3.

A. Phase-contrast photomicrographs of MEF with exposure of puromycin (Puro: 0, 1, 2, 10, 50, and 100 μg/mL) for 3 days. Puromycin was added at 100% confluence.

B-D. Phase-contrast photomicrographs of hepatocytes (#2062) 3 days after exposure to 2 μg/mL puromycin. Puromycin was added when the cells reached confluence (Day 0) and removed 3 days after the addition (Day 3). The Day 4 image shows the cells 24 hours after puromycin removal (D).

E. Gene expression by qRT-PCR in puromycin-treated hepatocytes (#2061 and #2062). The data were normalized by the housekeeping UBC gene. From left to right: non-treated hepatocytes (Hep2061), puromycin-treated hepatocytes (Hep2061+puro), non-treated hepatocytes (Hep2062), and puromycin-treated hepatocytes (Hep2062+puro). Cells were treated with 2 μg/mL puromycin for 3 days. Each relative value was calculated with respect to non-treated cells. Error bars indicate the standard deviation (n=3). The student's T-test was performed for statistical analysis of two groups. *$p < 0.05$, **$p < 0.01$, ***$p < 0.001$.

Supplemental Figure 3. Details of gene expression analysis and karyotyping of puromycin-treated proliferating hepatocytes, related to Figure 4.

A. Gene expression by qRT-PCR in puromycin-treated hepatocytes (#2064) from passage 4 to 25. The data were normalized with the housekeeping UBC gene. The expression level of each gene at passage 2 was set to 1.0. Error bars indicate the standard deviation (n=3).

B. Karyotypes of puromycin-treated hepatocytes (#2064) at passage 24. About 80% of the hepatocytes showed 46XX and no major abnormalities were found.

Supplemental Figure 4. Hepatocyte selection with a low concentration (1 μg/mL) of puromycin, related to Figures 3 and 4.

A. Growth curves of hepatocytes treated with 1μg/mL puromycin (n=2, shown as green and yellow dots). Proliferative capacity was analyzed at each passage. Cells were passaged in the ratio of 1:4 for each passage. The cell numbers were calculated as an average of 50 counts at each point. "Population doubling" indicates the cumulative number of divisions of the cell population.

B. Phase-contrast photomicrographs of puromycin-treated hepatocytes (#2064) from passages 5, 7, 13, 21, and 25.

C. Microscopic view of hepatocytes (#2064) at passages 5, 13, and 25. HE stain.

D. Immunocytochemical analysis of puromycin-treated hepatocytes (#2064) with an antibody to Ki67 (cell proliferation marker).

E. A senescence-associated beta-galactosidase stain of puromycin-treated hepatocytes (#2064) at the indicated passages. The number of β-galactosidase-positive senescent cells increased at passage 25.

F. Karyotypes of puromycin-treated hepatocytes (#2064) at passage 24.

Supplemental Figure 5. Long-term analysis of hepatocytes selected with a low concentration (1 µg/mL) of puromycin, related to Figures 3 and 4.

A. Gene expression by qRT-PCR in hepatocytes (#2064) at passage 4, 11, and 17. From left to right: non-treated hepatocytes (Hep2061), puromycin-treated hepatocytes (Hep2061+puro), non-treated hepatocytes (Hep2062), and puromycin-treated hepatocytes (Hep2062+puro). The data were normalized by the housekeeping UBC gene. The expression level of each gene at passage 2 was set to 1.0. Error bars indicate the standard deviation (n=3). The student's T-test was performed for statistical analysis of two groups. *$p < 0.05$, **$p < 0.01$, ***$p < 0.001$.

B. Gene expression by qRT-PCR in puromycin-treated hepatocytes (#2064) from passage 4 to 25. Data were normalized with the housekeeping UBC gene. The expression level of each gene at passage 2 was set to 1.0. Error bars indicate the standard deviation (n=3).

C-E. Immunocytochemical analysis of puromycin-treated hepatocytes (#2064) at a low concentration ((1µg/mL) with antibodies to ALB (C), HNF4A (D), and bile duct marker CK7 (E) at the early and late passages (passage 5 and 25, respectively). Yellow arrows indicate binuclear cells (E).

F-G. Glycogen storage in puromycin-treated hepatocytes (passage 5, 13, and 25) by PAS stain with (F) and without (G) diastase digestion.

H-J. Expression of the genes for CYP1A2 (H), CYP2B6 (I), and CYP3A4 (J) in puromycin-treated hepatocytes after exposure to omeprazole (H), phenobarbital (I), or rifampicin (J). The expression level of each gene without any treatment (DMSO) was set to 1.0. Each expression level was calculated from the results of independent (biological) triplicate experiments. Error bars indicate the standard error (n=3). The student's T-test was performed for statistical analysis of two groups. *$p < 0.05$.

K. CYP3A4 activity of hepatocytes (passage 5, 11, and 25). The CYP3A4 activity of HepG2 cells was set to 1.0. Error bars represent the standard errors (n=3). Each expression level was calculated from the results of independent (biological) triplicate experiments. Error bars indicate the standard error (n=3). **$p < 0.01$.

Supplemental Figure 6. Detail of expression analysis and comprehensive analysis of hepatic progenitor cell markers in proliferating hepatocytes, related to Figure 5.

A, B. Gene expression of the genes for hepatic progenitor cell markers by qRT-PCR in non-treated (A) and puromycin-treated (B) hepatocytes (#2064). Data were normalized with the housekeeping UBC gene. The expression level of each gene in HepG2 cells was set to 1.0. Error bars indicate the standard deviation (n=3).

C. Immunocytochemical analysis of non-treated and puromycin-treated hepatocytes (#2064) with antibodies to AFP and CK19 at the early passage (passage 5).

D-F. Gene sets enriched in either (FDR < 0.05) compared to non-treated and puromycin-treated hepatocytes (#2064). Gene sets for the TCA cycle and pentose phosphate circuit (D), mitophagy (E), and gene sets related to epithelial-mesenchymal transition (EMT) (F) were identified. "non": non-treated hepatocytes (#2064), "+puro": puromycin-treated hepatocytes (#2064).

G. Heatmap of genes whose expression is up-regulated during the epithelial-mesenchymal transition in non-treated and puromycin-treated hepatocytes (#2064) (gene list: https://journals.plos.org/plosone/article?id=10.1371/journal.pone.0051136). The color bars show the signal strength in scaled by z score. "non treated": non-treated hepatocytes (#2064), "+puro": puromycin-treated hepatocytes (#2064) .

Supplemental Figure 7. Hepatocytes treated with low concentrations (1 μg/mL) of puromycin restore the expression level of liver-related genes after long-term culture to the level of the initial stage of hepatocyte culture, related to Figure 6 and 7.

A. Hepatic maturation protocol. Hepatocytes at early passage (Passage 5), middle passage (Passage 11), and late passage (Passage 25) at 70% confluence were exposed to 1 or 2 μg/mL puromycin for 3 days. Hepatocytes were then seeded onto low adhesion plates for spheroid formation one day after removal of puromycin. The cells were cultured at a form of spheroid for 10 days, and applied to further analysis.

B-J. Histology of spheroids generated from hepatocytes (#2064) at each passage (B, E, F: Early passage (Passage 5); C, G, H: middle passage (Passage 11); D, I, J: late passage (Passage 25)). "+puro (x1)": Spheroids generated from hepatocytes (#2064) treated with 1 μg/ml puromycin. B to D: HE stain; E, G, I: PAS stain; F, H, J: PAS stain used in combination with diastase, an enzyme that breaks down glycogen.

K-M. Immunohistochemistry of spheroids generated from puromycin-treated hepatocytes (#2064) at each passage (K: Early passage (passage 5); L: middle passage (passage 11); M: late passage (passage 25)) with antibodies to albumin (ALB), cytochrome p450 3A4 (CYP3A4), and multidrug resistance-associated protein 2 (MRP2). "+puro (x1)": Spheroids generated from hepatocytes (#2064) treated with 1 μg/ml puromycin.

Supplemental Figure 8. Hepatocytes treated with low concentrations (1 μg/mL) of puromycin restore the expression level of liver-related genes after long-term culture to the level of the initial stage of hepatocyte culture, related to Figure 6 and 7.

Gene expression levels were analyzed by qRT-PCR. Puromycin-treated hepatocytes (#2064) were applied to spheroid culture for 10 days (Figure S7A). RNAs were isolated from spheroid generated from puromycin-treated hepatocytes (#2064) at passage 5 (A), passage 11 (B), and passage 25 (C). The data were normalized by the housekeeping UBC gene. The expression level of each gene in hepatocytes (#2064) without any treatment at passage 2 was set to 1.0. "U.D.": undetectable. Each expression level was calculated from the results of independent (biological) triplicate experiments. Error bars indicate the standard error. The student's T-test was performed for statistical analysis of two groups. *$p < 0.05$, **$p < 0.01$, ***$p < 0.001$.

Table 2. Primers used for qRT-PCR

Gene	Forward (5' to 3')	Reverse (5' to 3')
AAT	GGGAAACTACAGCACCTGGA	CCCCATTGCTGAAGACCTTA
AFP	AGCTTGGTGGTGGATGAAAC	CCCTCTTCAGCAAAGCAGAC
ALB	TGGCACAATGAAGTGGGTAA	CTGAGCAAAGGCAATCAACA
ASMA	CAGCCAAGCACTGTCAGG	CCAGAGCCATTGTCACACAC
CK19	TCGAAGGCCTGAAGGAAGAGC	ACCTCCCGGTTCAATTCTTCAG
CK7	GAGGTCACCATTAACCAGAGCC	GCAATCTGGGCCTCAAAGATGT
COL1A1	CACACGTCTCGGTCATGGTA	AAGAGGAAGGCCAAGTCGAG
CPS1	CAAGTTTTGCAGTGGAATCG	GGACAGATGCCTGAGCCTAA
CYP1A2	CAATCAGGTGGTGGTGTCAG	GCTCCTGGACTGTTTTCTGC
CYP2B6	TCCTTTCTGAGGTTCCGAGA	TCCCGAAGTCCCTCATAGTG
CYP2C9	AGATACATTGACCTTCTCCCC	GCTTCTCCCACACAAATCC
CYP3A4	CAAGACCCCTTTGTGGAAAA	CGAGGCGACTTTCTTTCATC
EpCAM	GTCTAAAAGCTGGTGTTATTGC	TCTCACCCATCTCCTTTATCTC
OTC	TTTCCAAGGTTACCAGGTTACAA	CTGGGCAAGCAGTGTAAAAAT
PROM1	ATTCACCAGCAACGAGTCC	CTCTCTCCAACAATCCATTCC

SOX9	GACTACACCGACCACCAGAACTCC	GTCTGCGGGATGGAAGGGA
UBC	GGAGCCGAGTGACACCATTG	CAGGGTACGACCATCTTCCAG

Table 3. Antibodies used for immunohistochemistry

Antibody	Species	Catalog #	Dilution	Manufacturer
ki67	Rabbit	ab15580	1:500	Abcam
ALB	Goat	A80-229A	1:100	Bethyl Laboratories
AFP	Rabbit	sc-15375	1:250	Santa Cruz
HNF4A	Mouse	sc-374229	1:200	Santa Cruz
CK7	Mouse	M7018	1:250	Dako
CK19	Mouse	sc-6278	1:250	Santa Cruz
MRP2	Rabbit	ab172630	1:100	Abcam
CYP3A4	Goat	sc-27639	1:100	Santa Cruz

Table 4. secondary antibodies used for immunohistochemistry

Antibody	Manufacturer	Catalog #
Alexa Fluor 488 rabbit anti-goat IgG	Invitrogen	A11078
Alexa Fluor 488 goat anti-rabbit IgG	Invitrogen	A11008
Alexa Fluor 488 goat anti-mouse IgG	Invitrogen	A21121
Alexa Fluor 546 goat anti-mouse IgG1	Invitrogen	A21123
Alexa Fluor 568 goat anti-mouse IgG2a	Invitrogen	A21134

REFERENCE

1. Gissen P, Arias IM. Structural and functional hepatocyte polarity and liver disease. J Hepatol. 2015;63: 1023–1037.

2. Ponsoda X, Pareja E, Gómez-Lechón MJ, Fabra R, Carrasco E, Trullenque R, et al. Drug biotransformation by human hepatocytes. In vitro/in vivo metabolism by cells from the same donor. J Hepatol. 2001;34: 19–25.

3. Gómez-Lechón MJ, Donato MT, Castell JV, Jover R. Human hepatocytes as a tool for studying toxicity and drug metabolism. Curr Drug Metab. 2003;4: 292–312.

4. Dhawan A, Puppi J, Hughes RD, Mitry RR. Human hepatocyte transplantation: current experience and future challenges. Nat Rev Gastroenterol Hepatol. 2010;7: 288–298.

5. Collins SD, Gastoenterology and Liver Laboratory, Ingham Institute for Applied Medical Research, Liverpool, New South Wales, Australia, et al. In Vitro Models of the Liver: Disease Modeling, Drug Discovery and Clinical Applications. Hepatocellular Carcinoma. 2019. pp. 47–67. doi:10.15586/hepatocellularcarcinoma.2019.ch3

6. Chen M, Suzuki A, Borlak J, Andrade RJ, Lucena MI. Drug-induced liver injury: Interactions between drug properties and host factors. J Hepatol. 2015;63: 503–514.

7. Kang L-I, Mars WM, Michalopoulos GK. Signals and cells involved in regulating liver regeneration. Cells. 2012;1: 1261–1292.

8. Miyajima A, Tanaka M, Itoh T. Stem/progenitor cells in liver development, homeostasis, regeneration, and reprogramming. Cell Stem Cell. 2014;14: 561–574.

9. Li W, Li L, Hui L. Cell Plasticity in Liver Regeneration. Trends Cell Biol. 2020;30: 329–338.

10. Kopp JL, Grompe M, Sander M. Stem cells versus plasticity in liver and pancreas regeneration. Nat Cell Biol. 2016;18: 238–245.

11. Gilgenkrantz H, Collin de l'Hortet A. Understanding Liver Regeneration: From Mechanisms to Regenerative Medicine. Am J Pathol. 2018;188: 1316–1327.

12. Michalopoulos GK, Bhushan B. Liver regeneration: biological and pathological mechanisms and implications. Nat Rev Gastroenterol Hepatol. 2021;18: 40–55.

13. Tarlow BD, Pelz C, Naugler WE, Wakefield L, Wilson EM, Finegold MJ, et al. Bipotential adult liver progenitors are derived from chronically injured mature hepatocytes. Cell Stem Cell. 2014;15: 605–618.

14. Tanimizu N, Nishikawa Y, Ichinohe N, Akiyama H, Mitaka T. Sry HMG box protein 9-positive (Sox9+) epithelial cell adhesion molecule-negative (EpCAM-) biphenotypic cells derived from hepatocytes are involved in mouse liver regeneration. J Biol Chem. 2014;289: 7589–7598.

15. Lu W-Y, Bird TG, Boulter L, Tsuchiya A, Cole AM, Hay T, et al. Hepatic progenitor cells of biliary origin with liver repopulation capacity. Nat Cell Biol. 2015;17: 971–983.

16. Deng X, Zhang X, Li W, Feng R-X, Li L, Yi G-R, et al. Chronic Liver Injury Induces Conversion of Biliary Epithelial Cells into Hepatocytes. Cell Stem Cell. 2018;23: 114–122.e3.

17. Schmidt LE, Dalhoff K. Alpha-fetoprotein is a predictor of outcome in acetaminophen-induced liver injury. Hepatology. 2005;41: 26–31.

18. Katsuda T, Kawamata M, Hagiwara K, Takahashi R-U, Yamamoto Y, Camargo FD, et al. Conversion of Terminally Committed Hepatocytes to Culturable Bipotent Progenitor Cells with Regenerative Capacity. Cell Stem Cell. 2017;20: 41–55.

19. Wu H, Zhou X, Fu G-B, He Z-Y, Wu H-P, You P, et al. Reversible transition between hepatocytes and liver progenitors for in vitro hepatocyte expansion. Cell Res. 2017;27: 709–712.

20. Zhang K, Zhang L, Liu W, Ma X, Cen J, Sun Z, et al. In Vitro Expansion of Primary Human Hepatocytes with Efficient Liver Repopulation Capacity. Cell Stem Cell. 2018;23: 806–819.e4.

21. Katsuda T, Matsuzaki J, Yamaguchi T, Yamada Y, Prieto-Vila M, Hosaka K, et al. Generation of human hepatic progenitor cells with regenerative and metabolic capacities from primary hepatocytes. Elife. 2019;8. doi:10.7554/eLife.47313

22. Yarmolinsky MB, Haba GL. INHIBITION BY PUROMYCIN OF AMINO ACID INCORPORATION INTO PROTEIN. Proc Natl Acad Sci U S A. 1959;45: 1721–1729.

23. Miyamoto-Sato E, Nemoto N, Kobayashi K, Yanagawa H. Specific bonding of puromycin to full-length protein at the C-terminus. Nucleic Acids Res. 2000;28: 1176–1182.

24. Aviner R. The science of puromycin: From studies of ribosome function to applications in biotechnology. Comput Struct Biotechnol J. 2020;18: 1074–1083.

25. Enosawa S. Isolation of GMP Grade Human Hepatocytes from Remnant Liver Tissue of Living Donor Liver Transplantation. In: Stock P, Christ B, editors. Hepatocyte Transplantation: Methods and Protocols. New York, NY: Springer New York; 2017. pp. 231–245.

26. Enosawa S, Horikawa R, Yamamoto A, Sakamoto S, Shigeta T, Nosaka S, et al. Hepatocyte transplantation using a living donor reduced graft in a baby with ornithine transcarbamylase deficiency: a novel source of hepatocytes. Liver Transpl. 2014;20: 391–393.

27. Sugahara G, Yamasaki C, Yanagi A, Furukawa S, Ogawa Y, Fukuda A, et al. Humanized liver mouse model with transplanted human hepatocytes from patients with ornithine transcarbamylase deficiency. J Inherit Metab Dis. 2020. doi:10.1002/jimd.12347

28. Yachida S, Wood LD, Suzuki M, Takai E, Totoki Y, Kato M, et al. Genomic Sequencing Identifies ELF3 as a Driver of Ampullary Carcinoma. Cancer Cell. 2016;29: 229–240.

29. McCullough A. ROCK Inhibitor and Feeder Cells Induce the Conditional Reprogramming of Epithelial Cells. Yearbook of Pathology and Laboratory Medicine. 2013. pp. 289–290. doi:10.1016/j.ypat.2012.11.026

30. Nishimura K, Sano M, Ohtaka M, Furuta B, Umemura Y, Nakajima Y, et al. Development of defective and persistent Sendai virus vector: a unique gene delivery/expression system ideal for cell reprogramming. J Biol Chem. 2011;286: 4760–4771.

31. Kuroda K, Kiyono T, Isogai E, Masuda M, Narita M. Immortalization of fetal bovine colon epithelial cells by expression of human cyclin D1, mutant cyclin dependent kinase 4, and telomerase reverse …. PLoS. 2015. Available: https://journals.plos.org/plosone/article?id=10.1371/journal.pone.0143473

32. Tsuneishi R, Saku N, Miyata S, Javaregowda PK, Ite K, Toyoda M, et al. Ammonia-based enrichment and long-term propagation of zone I hepatocyte-like cells. doi:10.1101/2020.03.20.999680

33. Janda CY, Dang LT, You C, Chang J, de Lau W, Zhong ZA, et al. Surrogate Wnt agonists that phenocopy canonical Wnt and β-catenin signalling. Nature. 2017;545: 234–237.

34. Blobel G, Sabatini D. Dissociation of Mammalian Polyribosomes into Subunits by Puromycin. Proceedings of the National Academy of Sciences. 1971. pp. 390–394. doi:10.1073/pnas.68.2.390

35. Nathans D, Neidle A. Structural requirements for puromycin inhibition of protein synthesis. Nature. 1963;197: 1076–1077.

36. Steiner G, Kuechler E, Barta A. Photo-affinity labelling at the peptidyl transferase centre reveals two different positions for the A- and P-sites in domain V of 23S rRNA. EMBO J. 1988;7: 3949–3955.

37. Kirillov S, Porse BT, Vester B, Woolley P, Garrett RA. Movement of the 3′-end of tRNA through the peptidyl transferase centre and its inhibition by antibiotics. FEBS Letters. 1997. pp. 223–233. doi:10.1016/s0014-5793(97)00261-5

38. Li W, Yang L, He Q, Hu C, Zhu L, Ma X, et al. A Homeostatic Arid1a-Dependent Permissive Chromatin State Licenses Hepatocyte Responsiveness to Liver-Injury-Associated YAP Signaling. Cell Stem Cell. 2019. pp. 54–68.e5. doi:10.1016/j.stem.2019.06.008

39. Cicchini C, Amicone L, Alonzi T, Marchetti A, Mancone C, Tripodi M. Molecular mechanisms controlling the phenotype and the EMT/MET dynamics of hepatocyte. Liver Int. 2015;35: 302–310.

40. Xiang C, Du Y, Meng G, Soon Yi L, Sun S, Song N, et al. Long-term functional maintenance of primary human hepatocytes in vitro. Science. 2019;364: 399–402.

A

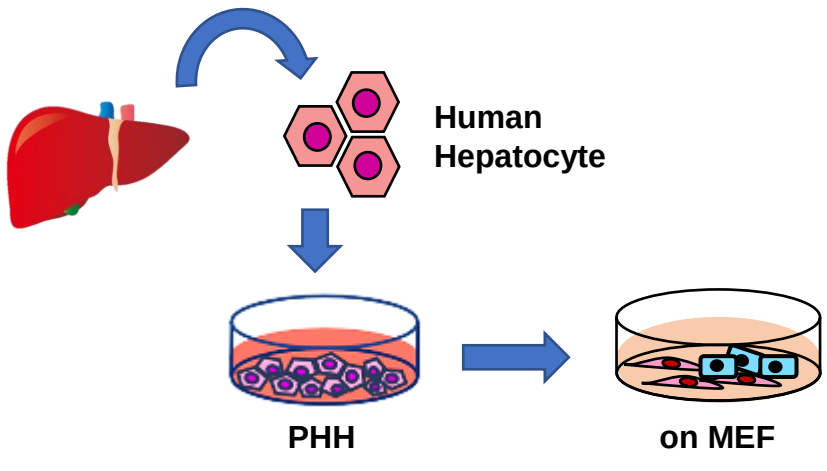

C

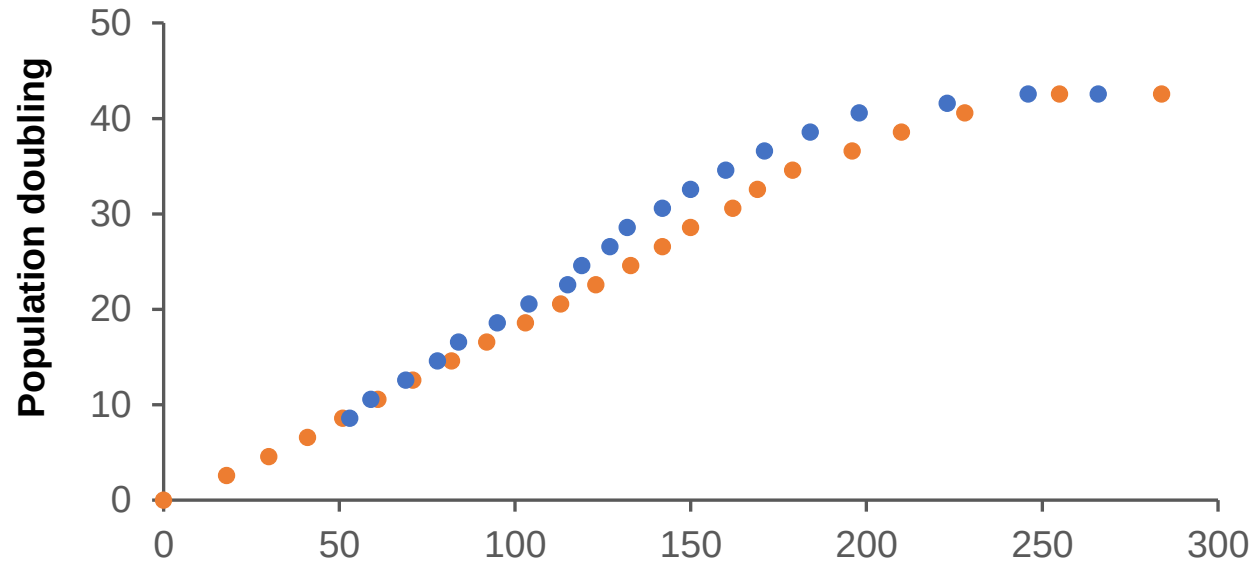

B

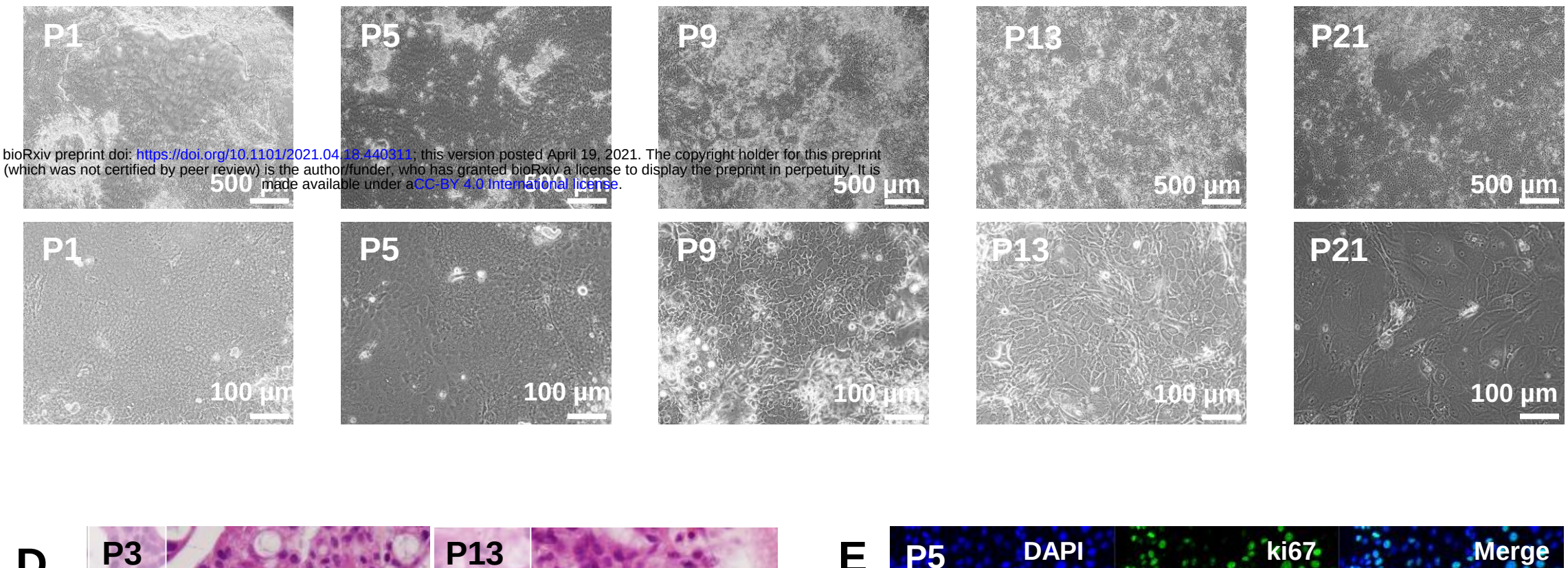

D

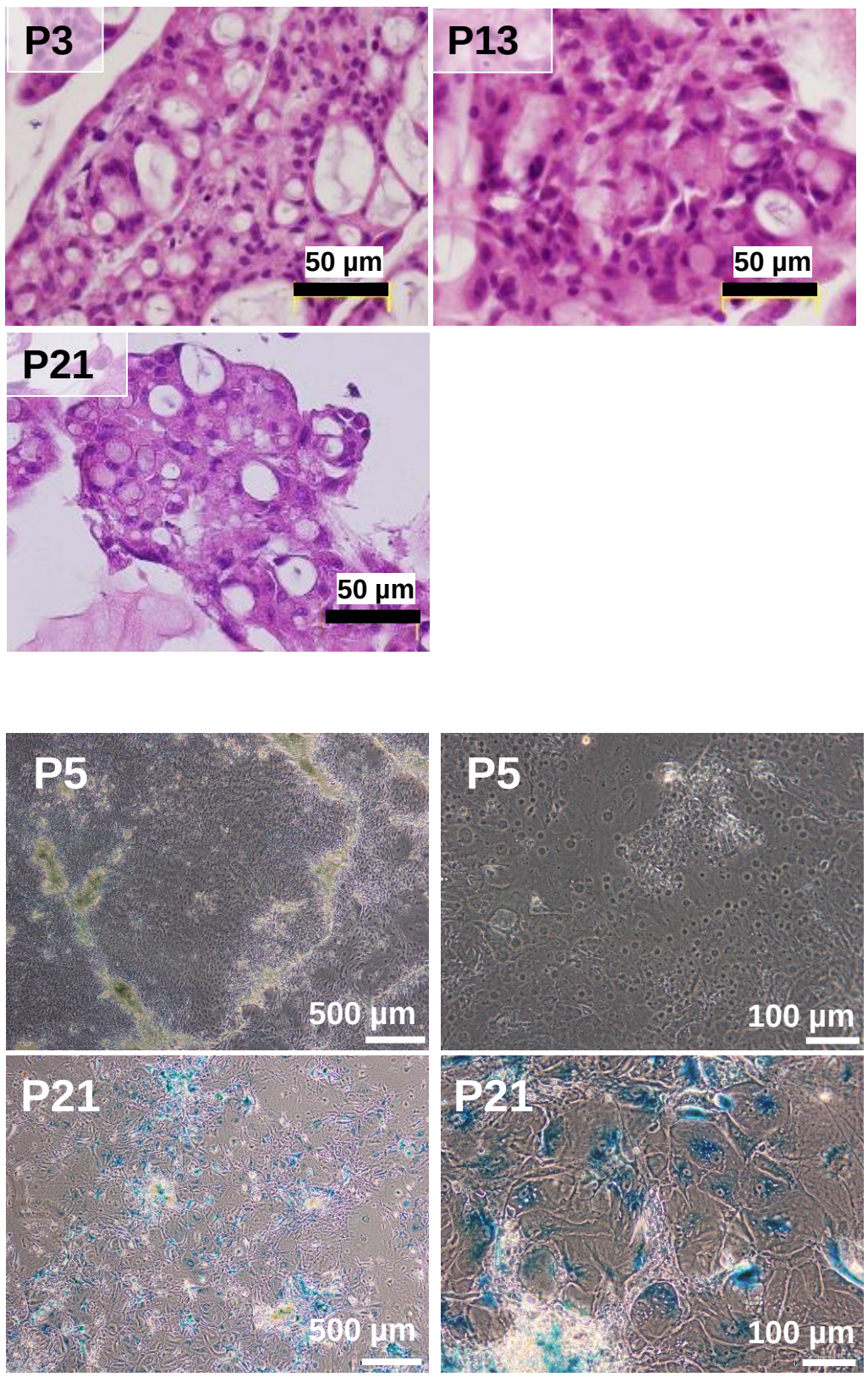

E

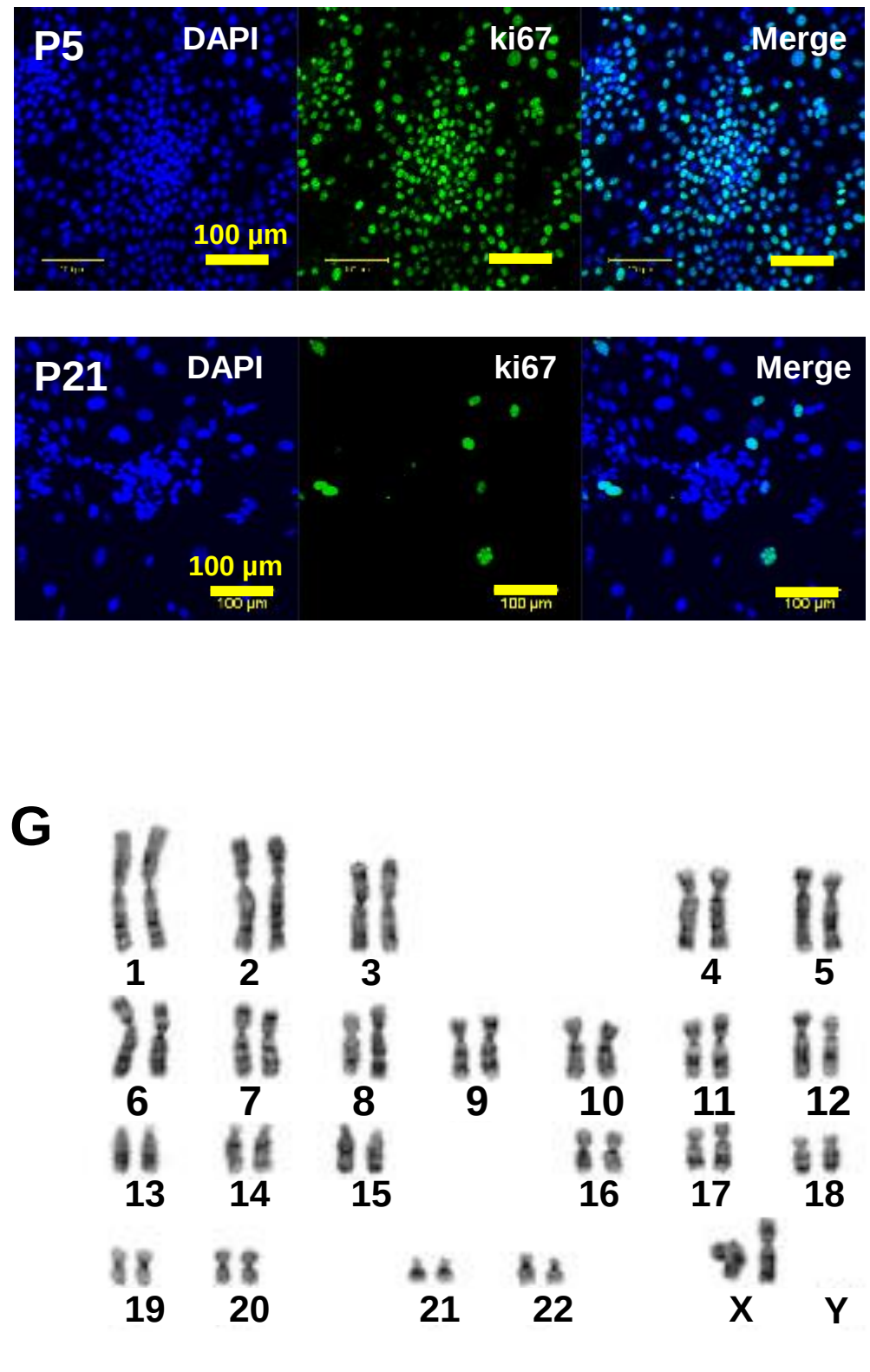

F

G

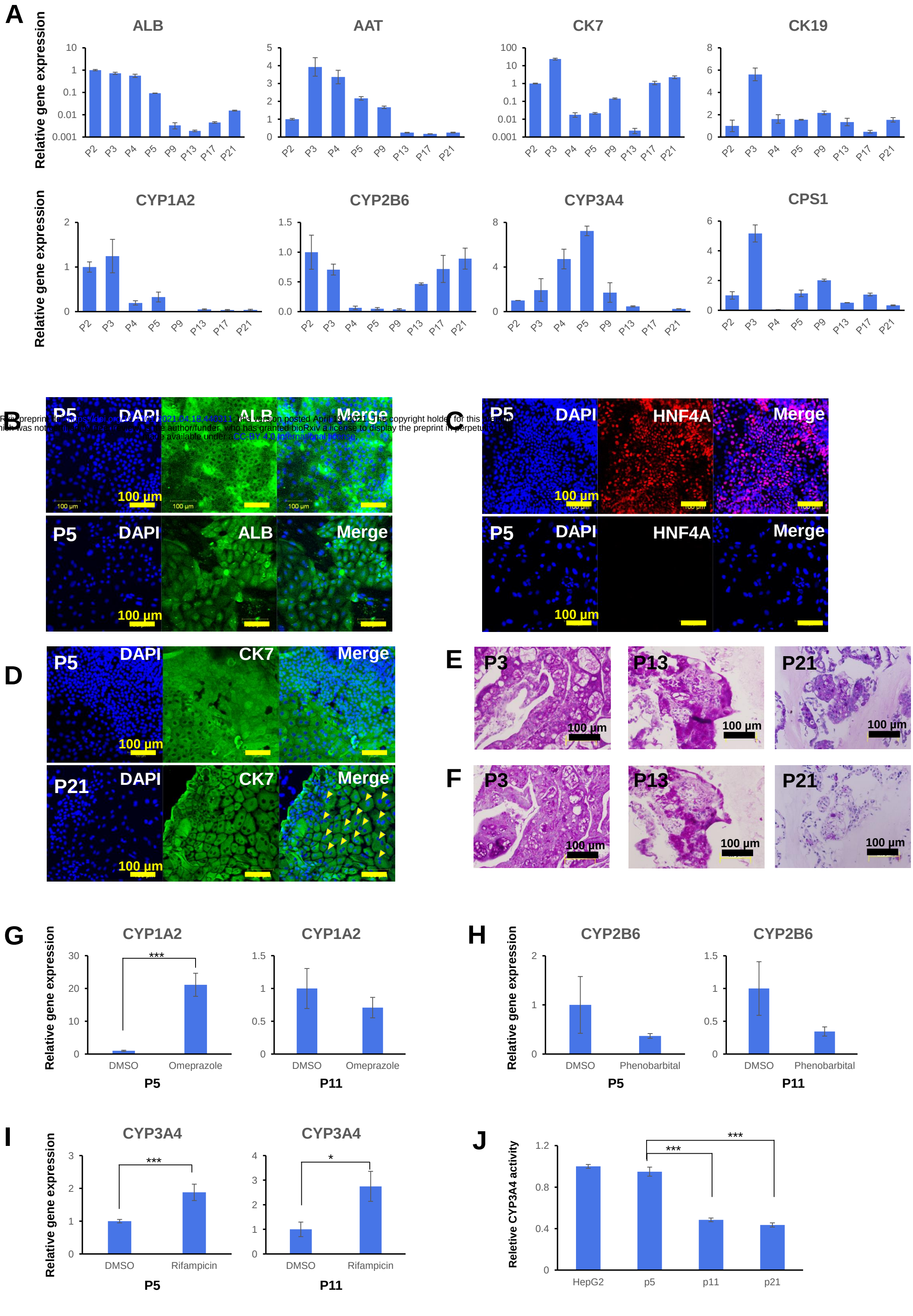

Fig3

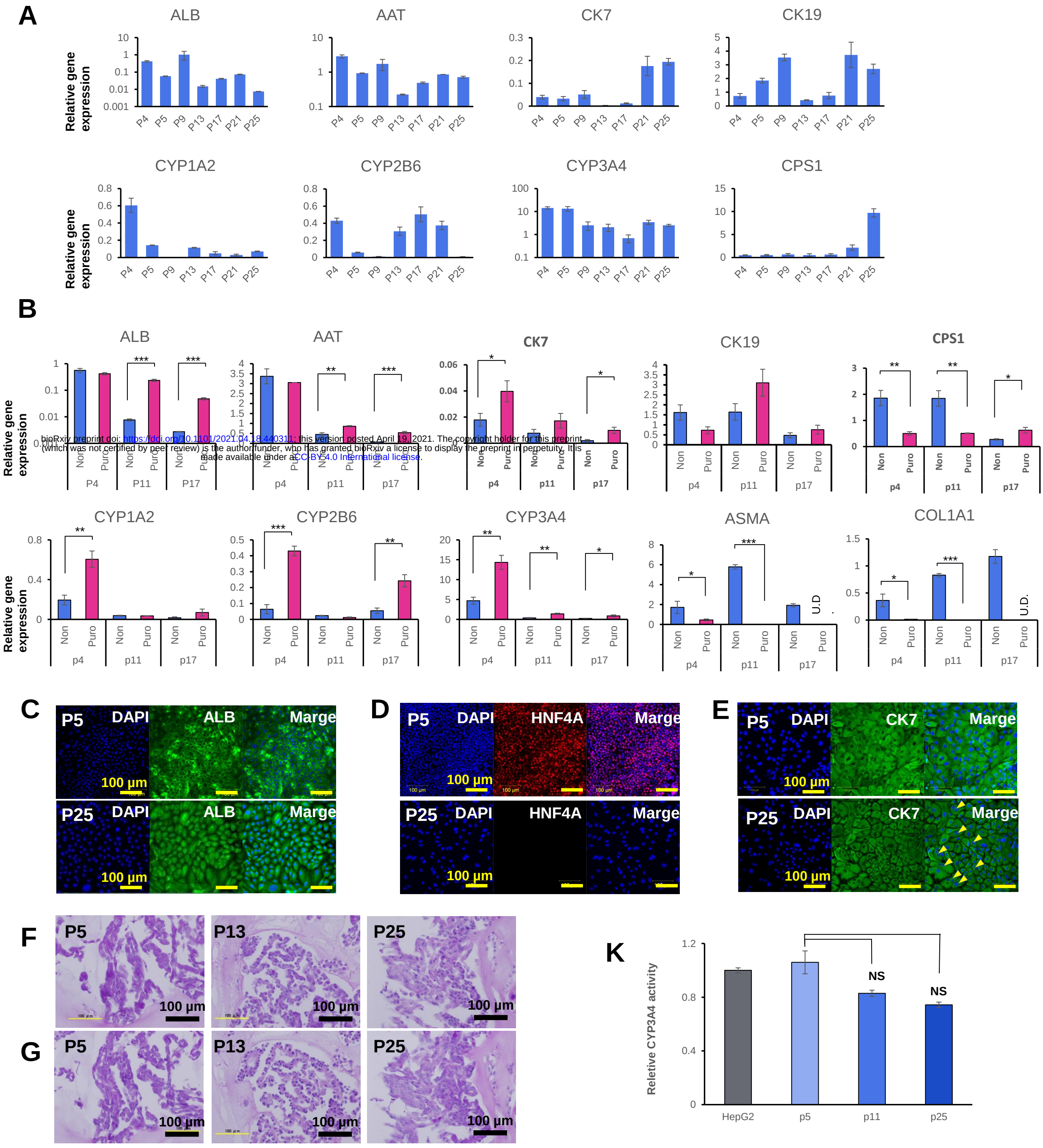

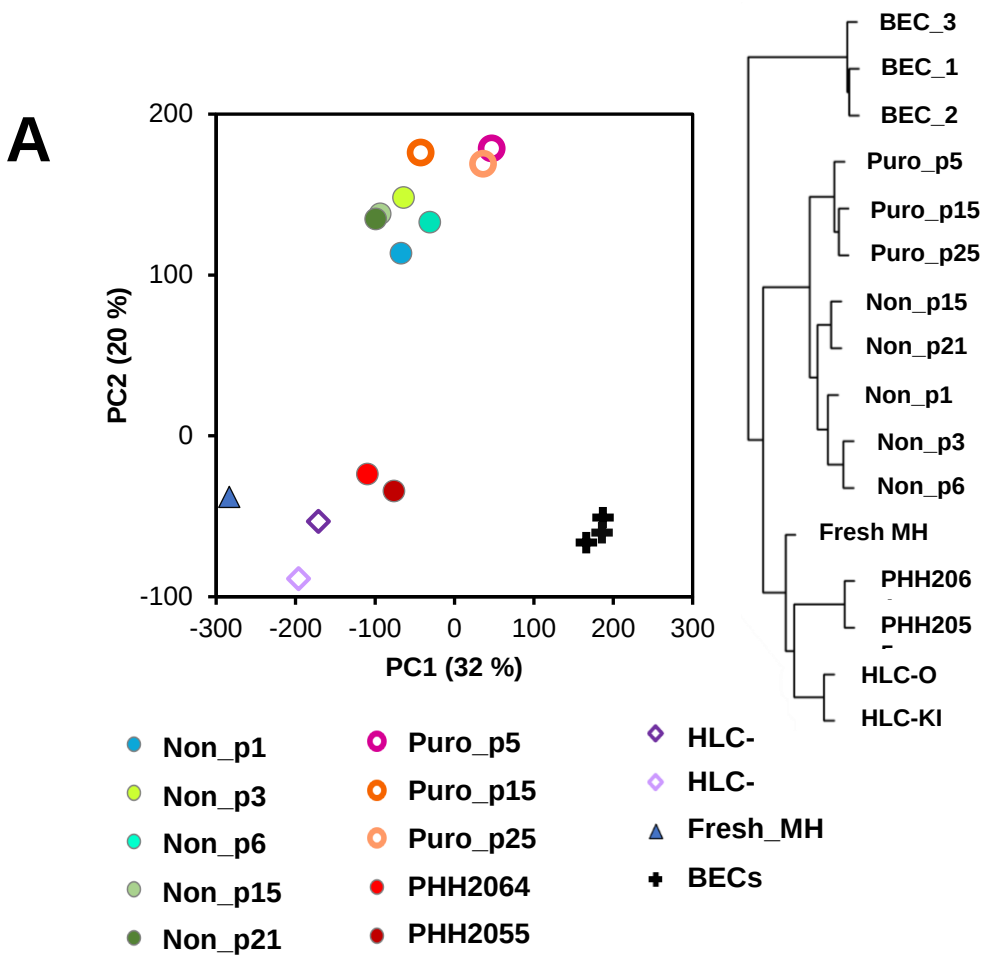

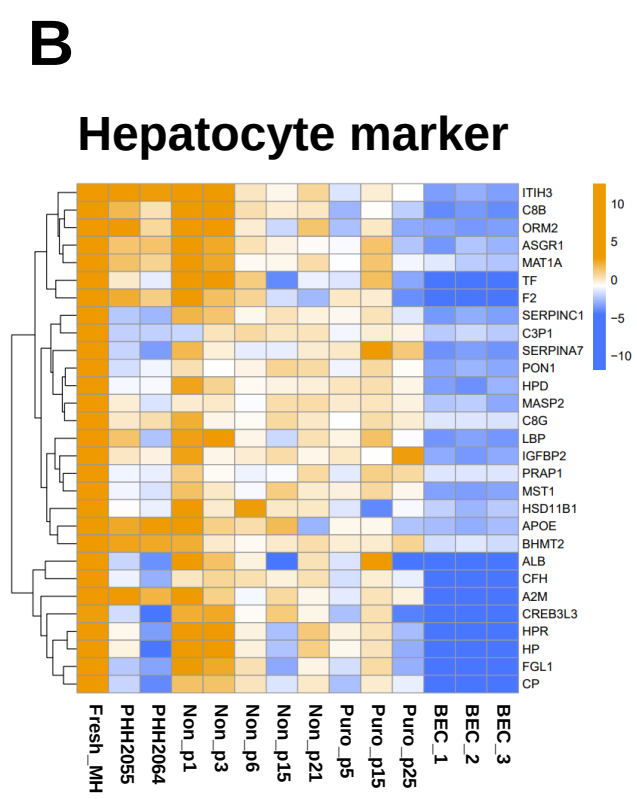

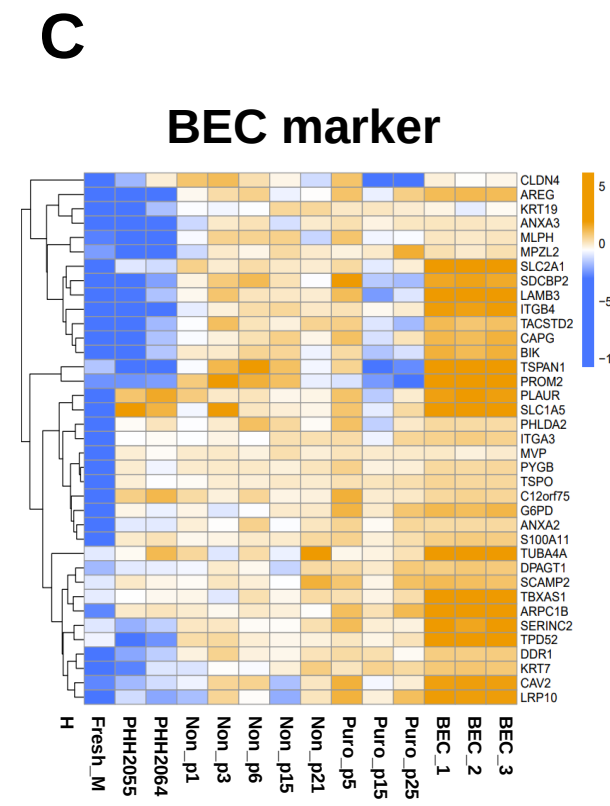

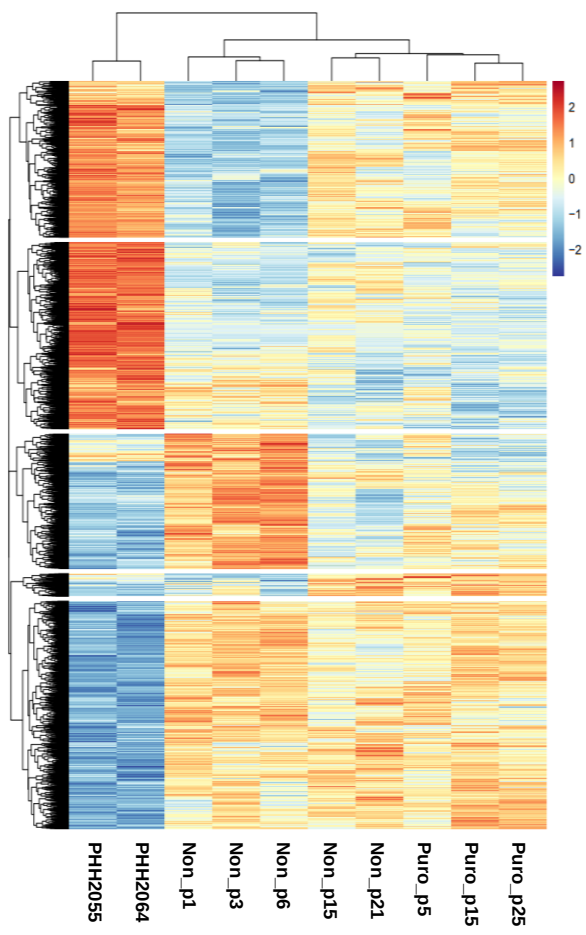

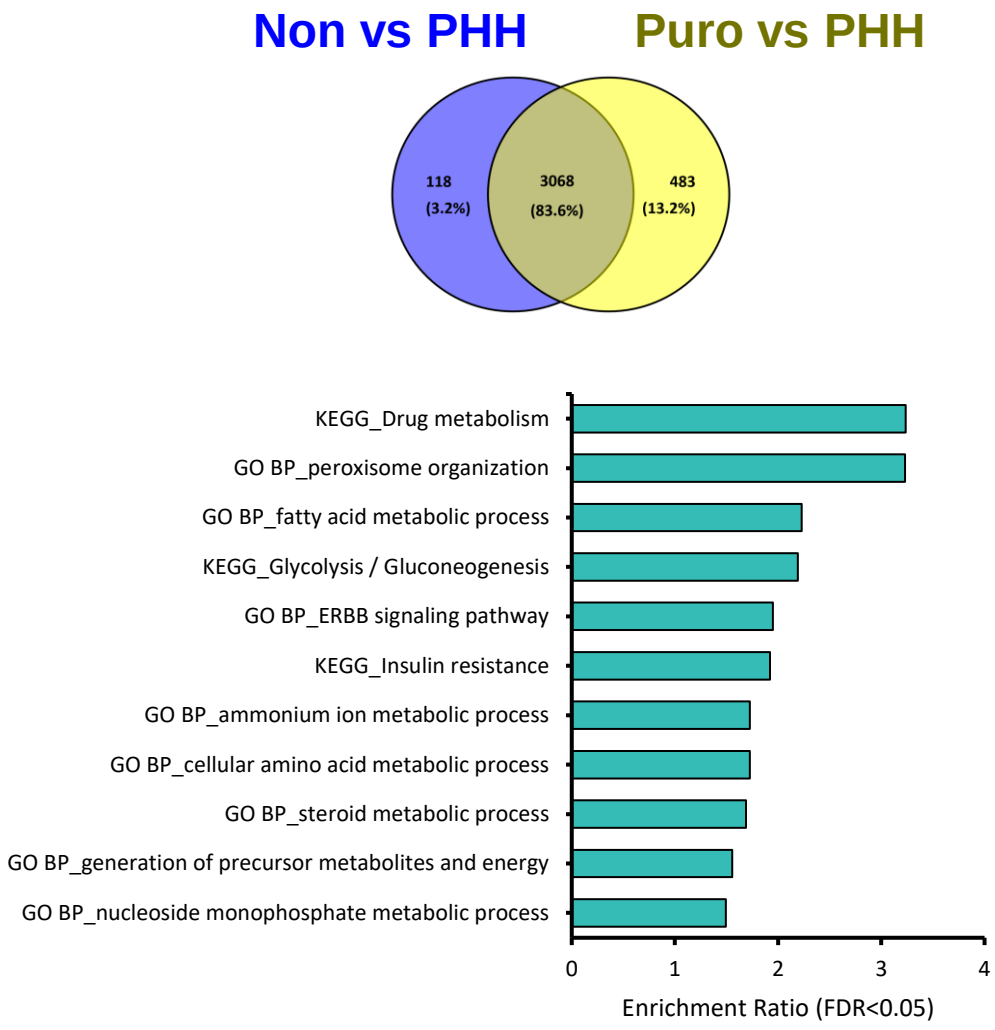

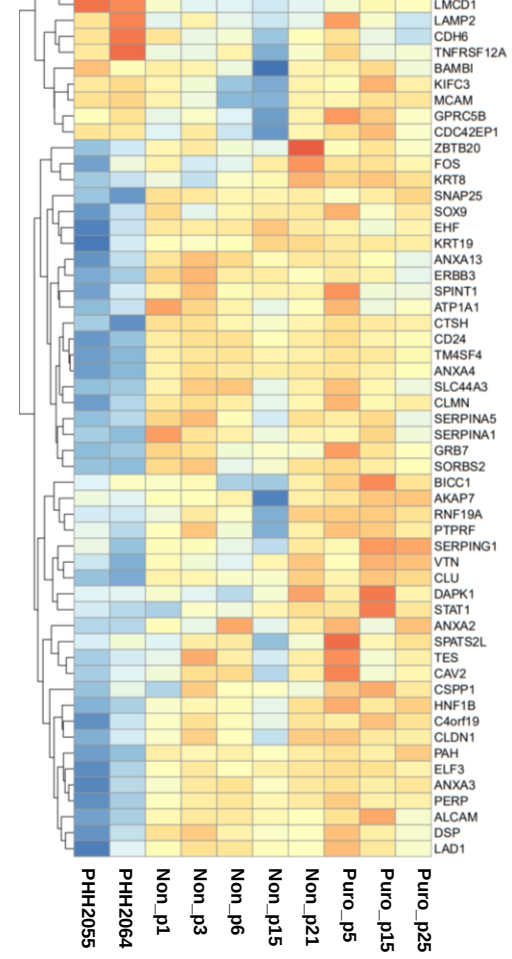

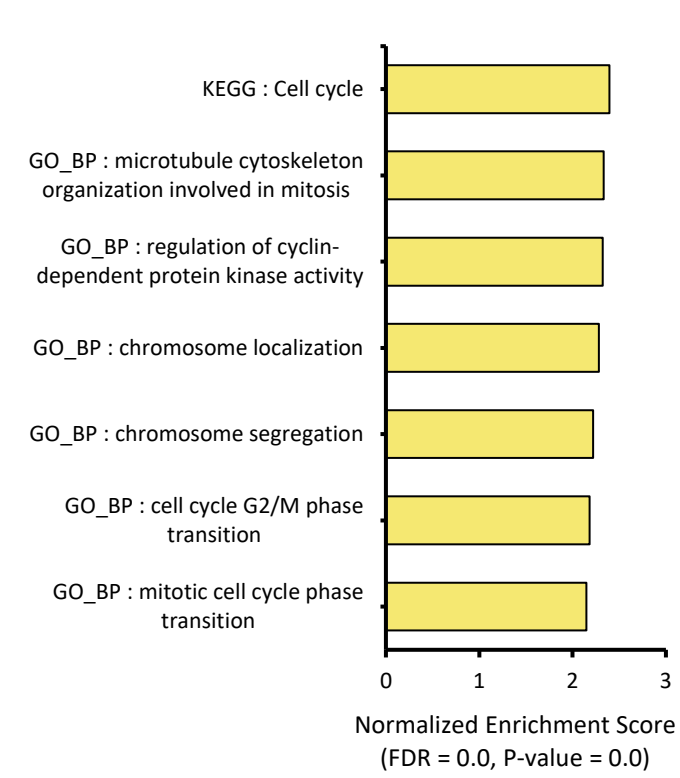

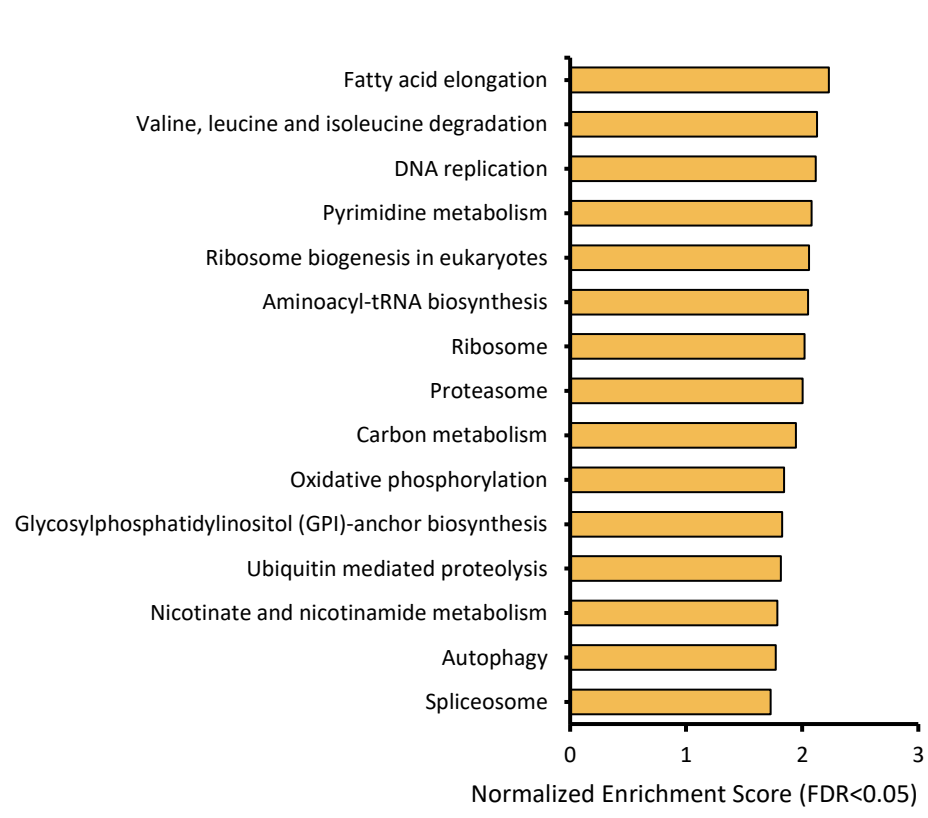

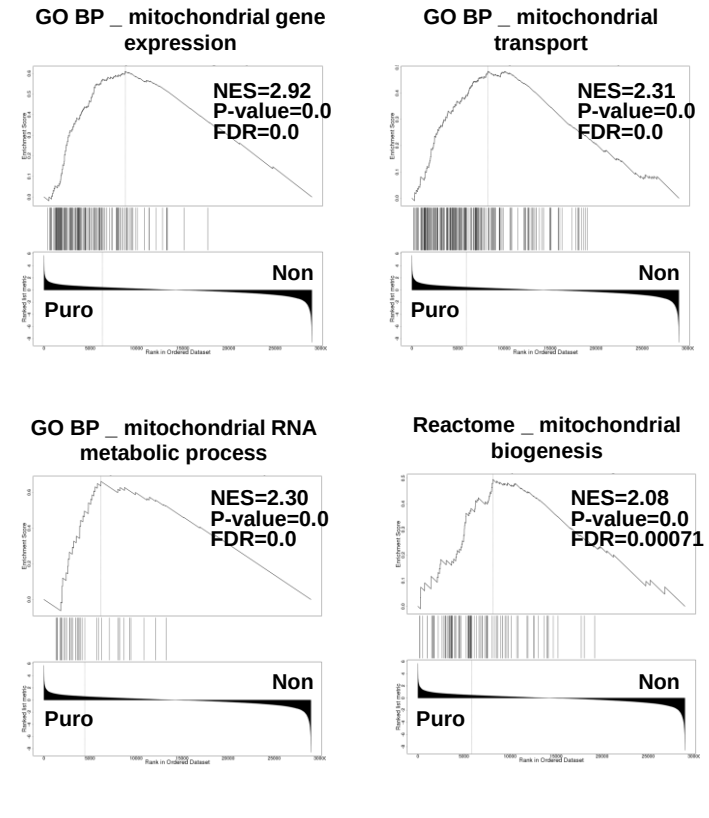

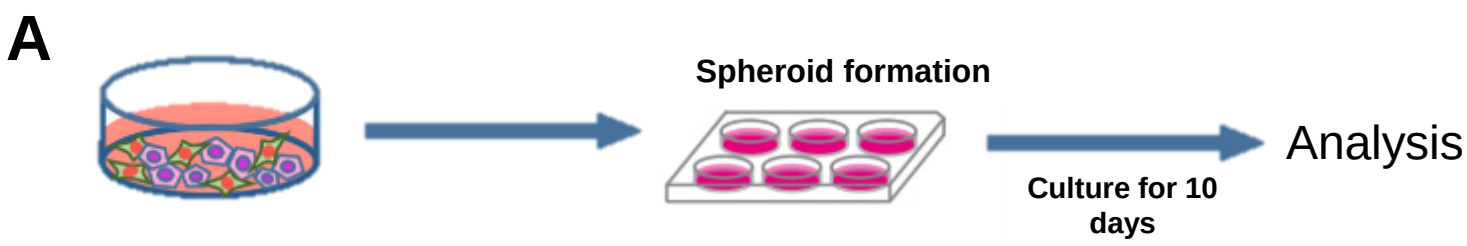

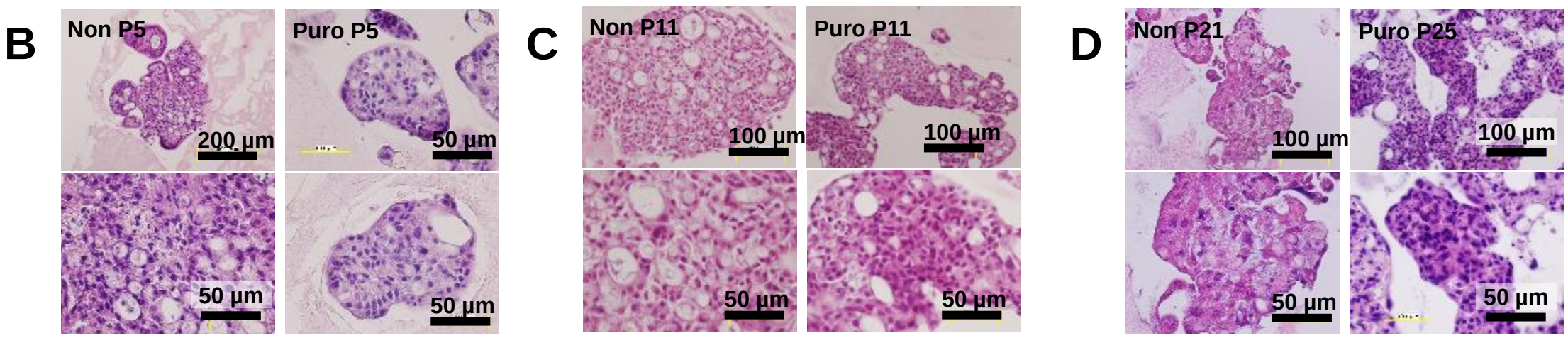

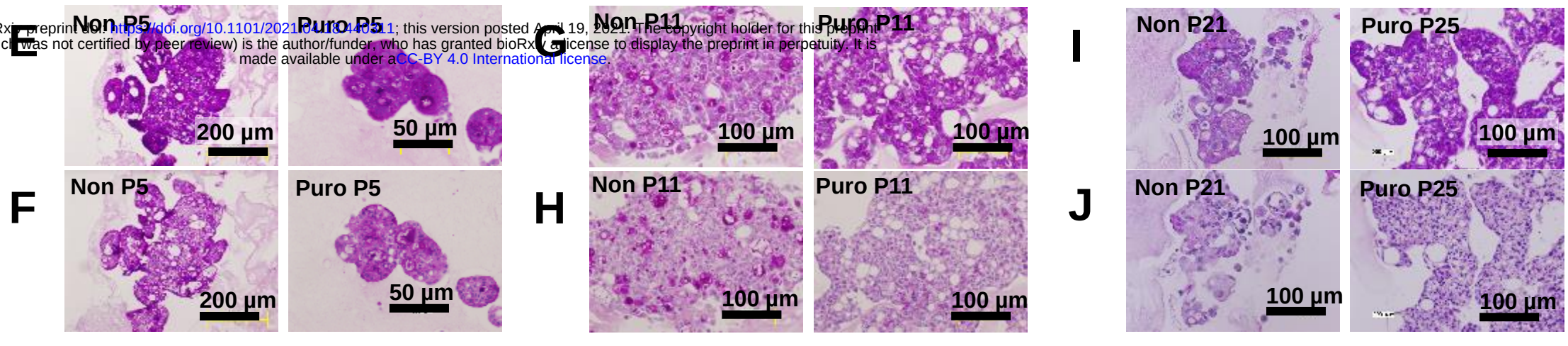

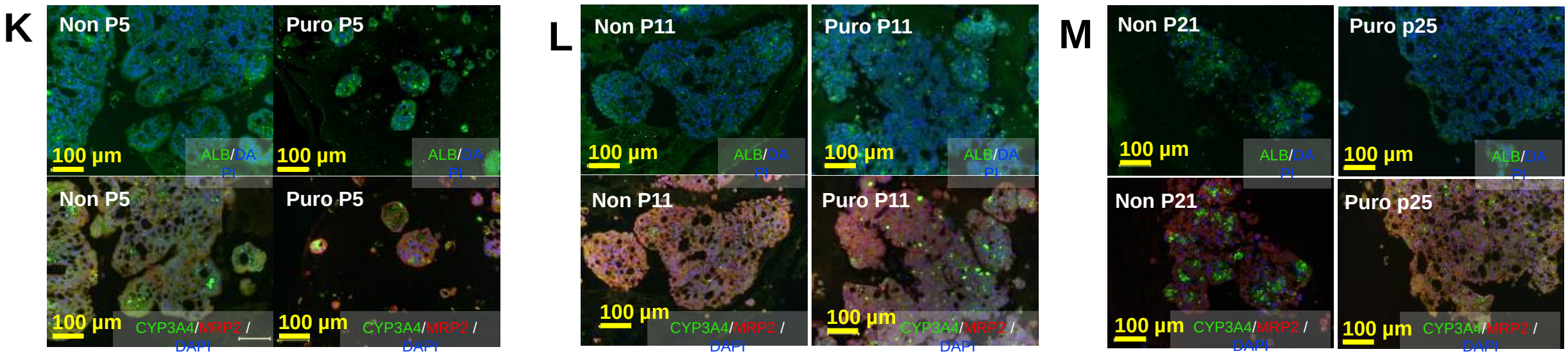

A

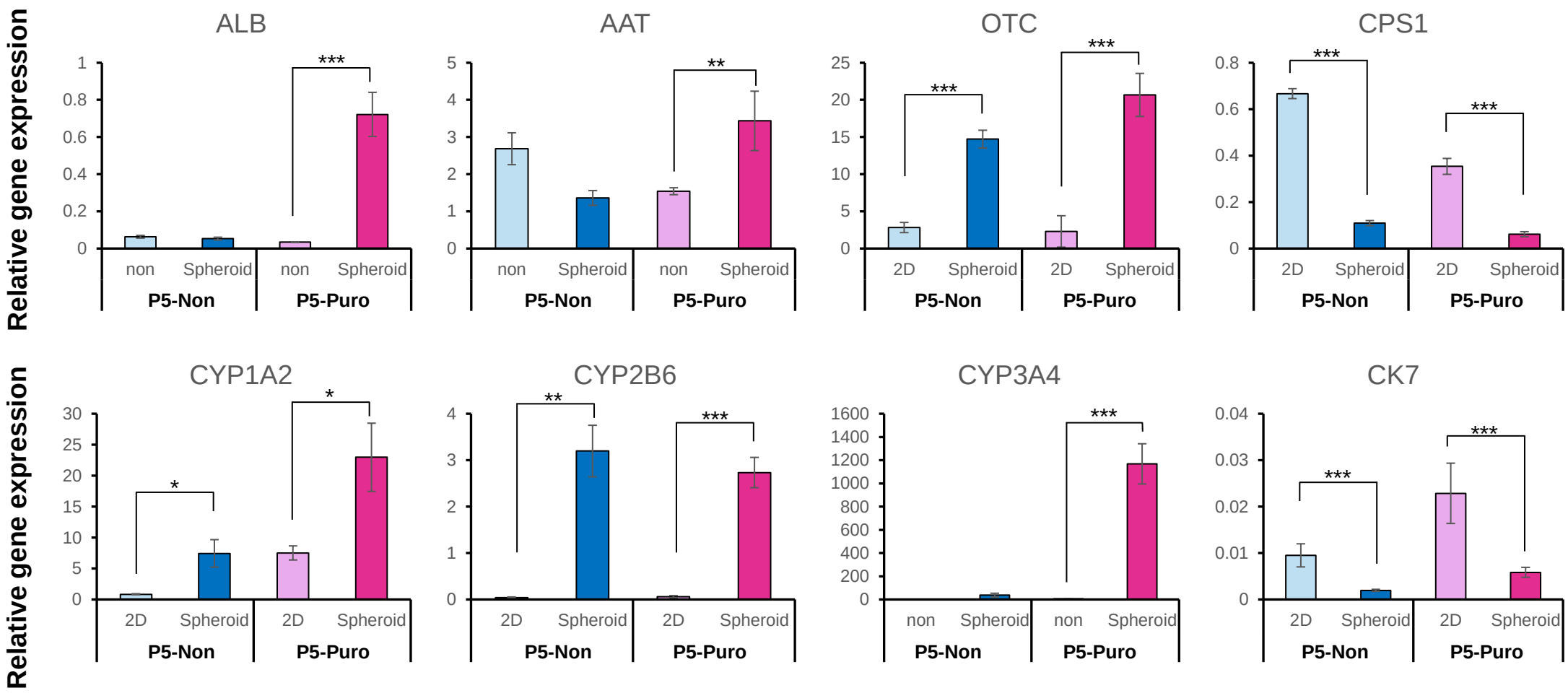

B

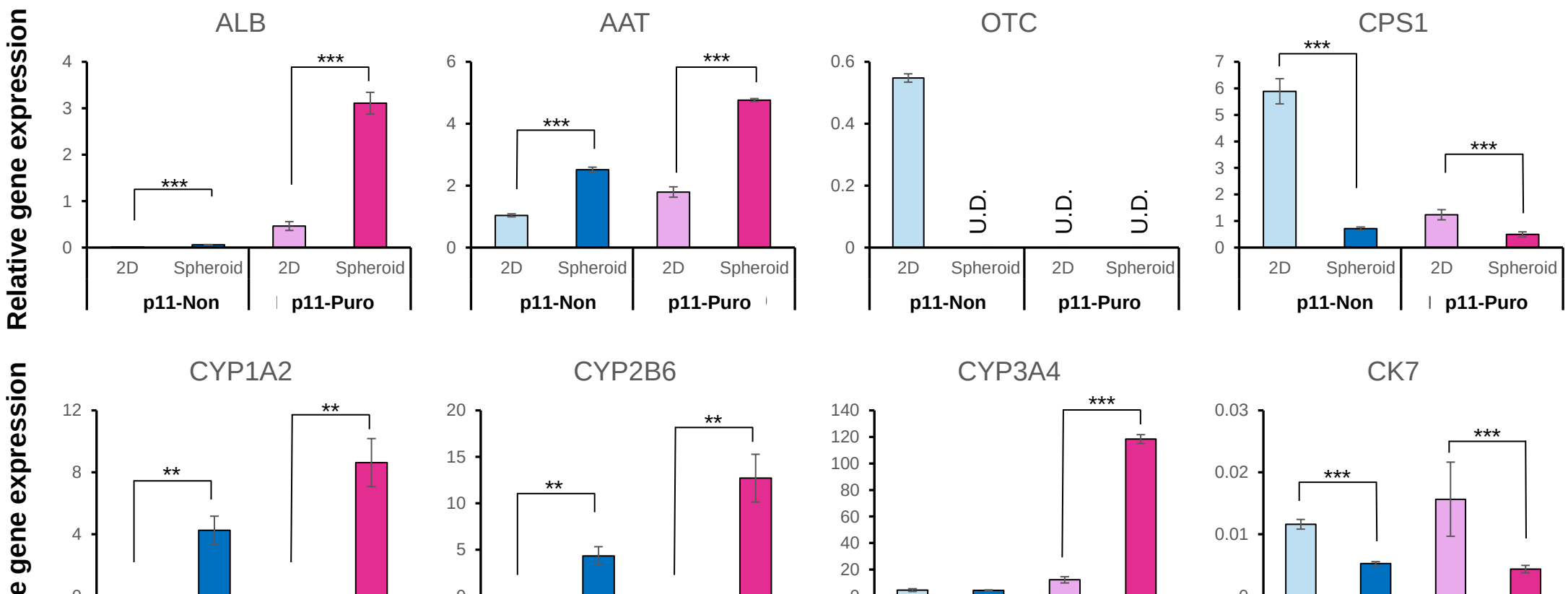

C